From the **Proceedings for the 37th Annual Symposium on Small Telescope Science June, 2018**

Investigation into the Accuracy of Small Telescope CCD Astrometry of Visual Double Stars

Skylar Larsen
Mt. Everest Academy
San Diego, CA
skylarlarsen@gmail.com

Schuyler Smith
San Diego High School of International Studies
San Diego, CA
schuyler.a.smith@gmail.com.

Jerry Hilburn
Boyce Research Initiatives and Education Foundation
Plumas Lake, CA
jerry@epsilonorion.com

Pat Boyce
Boyce Research Initiatives and Education Foundation
San Diego, CA
pat@boyce-astro.org

Abstract

Astrometric measurements using CCDs with small telescopes have become a routine means of observing and measuring visible double stars. Their measures are reported in the Journal of Double Star Observations and recorded in the Washington Double Star Catalog. Many factors ranging from telescope and camera characteristics to filters and seeing conditions affect the accuracy of these measurements. Researchers report here the results of observations of three rectilinear double stars and one 6th catalog orbital star that have varying but predicted separations and differences in magnitude. Over a three plus-month period, experienced operators made observations using 13 professional robotic telescope systems ranging in aperture from twelve to twenty-seven inches located around the world. Filters, airmass and exposure times were the independent variables applied to each set of observations for each system. Among the questions addressed, the impact of image saturation, camera resolution, telescope aperture, the stacking and averaging of images are addressed. Also presented are variations in the measurements for successive nights on the same telescope and optical train. Seven hundred observations were made. Experienced students then applied a single methodology for data reduction to all of the observations to eliminate the possible variations that these tools might cause. For a subset of observations, other experienced researchers performed the data reduction with other tools for comparison to the broad results to assess the accuracy of the baseline methodology used and to see if further research in the data reduction tools is warranted. Statistical results for all observations including standard deviation, mean error from "truth", and the standard error of the mean for all sets of data are computed and used to perform the analyses. Significant differences between the measured and the "true" separation and position angles are noted and suggestions for improved observation practices are made. A number of unexpected results were uncovered in this initial investigation. These results suggest a need for further investigations into in the methodology and reported accuracy of small telescope double star measurements using CCDs. The data will be publicly available and collaborations for future investigations are welcome.

1. Introduction

Boyce Research Initiatives and Education Foundation (BRIEF) in San Diego has been conducting double star seminars since 2015 in high schools, community colleges and online in San Diego (Boyce, 2017). Over forty papers reporting visual double star measurements made by student teams have been published or are in progress as of this date. The observations have been made by a variety of telescopes, CCD cameras and filters at the robotic sites around the globe offered by iTelescope and recently Las Cumbres Observatory. BRIEF has have encouraged students to use multiple observations to enable a statistical analysis of the data that is reported in the Journal of Double Star Observations (JDSO) and ultimately included in the Washington Double Star (WDS) catalog.

In every visual double star CCD observation conducted, questions such as these arise as to the accuracy of the measurements of separation (rho) and position angle (theta) and for planning the observations:

A. Does the filter used affect the measurement?
B. Does the exposure time and saturation significantly affect the accuracy?
C. How significant is the separation of the stars to measurement accuracy?
D. How influential is the difference in magnitude of the stars to the accuracy of the measurements?
E. Does the airmass or visual altitude for the observation affect the measurements?
F. How significant is the telescope aperture in the accuracy of the measurements?
G. How does the resolution of the camera affect the accuracy?
H. How many images should be taken for a good measurement?
I. Can you "average" together multiple different filters or should they be reported separately?
J. If observations are made on more than one night, can they be averaged together?
K. How many nights apart can observations be before they are sufficiently different to report them as separate measures?

It would seem that there are many factors that could affect the accuracy of measurements made with just one telescope. To design an observation plan to measure all these variables is challenging.

This investigation to undertaken to assess as many of these factors as possible. Observation plans began three times before succeeding with the last one described here. The first plan was to collect the data with one telescope with varying filters and air masses. This initial plan was to use recently and frequently measured visual doubles. The targets however did not offer the position certainty that was needed for "truth", a predictable correct theta and rho. Use of stars with and orbital or rectilinear solution would offer a recognized and predicted theta and rho. It was also discovered that doubles with a 3" to 6" separation could not be accurately measured and this category was removed from plans. The second plan addressed the "truth" requirement in target selection. The selected targets did not permit a low airmass and a high airmass observation from the same telescope in one night's observation run however. The selected targets needed to be further in the future to permit that part of the observation plan. Many observations were made but they were not suitable to address all the questions.

BRIEF had extensive time available on a rented 16" Ritchey Chrétien located at Sierra Remote Observatory (SRO) to conduct the tests. By the time the third observation plan was made, BRIEF had been awarded observation time as an Education Partner on the Las Cumbres Observatory worldwide network of identical 0.4m telescopes at six locations. Given this added dimension, BRIEF committed iTelescope time to the investigation as well. This added potentially eight more telescopes ranging in aperture from 3 inches to 27 inches from three sites around the world. Together this added the ability to make telescope to telescope, camera to camera, filter to filter, and location to location comparisons to refine the investigation and to address additional questions such as these:

L. Can observations from different observatories be averaged together if all other factors are equal?
M. Do the observatory locations matter?

Undaunted in adding to independent variables, researchers chose to proceed with these added telescope systems. BRIEF often reports data from widely varying systems, so curiosity as well as need won over in developing the third observation plan.

Mira Pro x64 and SAOImage DS9 were used for data reduction measurements in the past. An additional means of performing data reduction, Astro Image J (AIJ) became available over the past year. So, for good measure, a limited assessment of the effect of those three tools upon measurement accuracy was added.

N. To what extent do the data reduction tools used for CCD measurements affect measurement accuracy?

From experience it was known that the researchers could not expect 100% success with all intended observation runs. Researchers set out to collect data in a rational plan to address as many of the above questions as possible. Seven hundred successful observations were made with thirteen robotic telescopes. This paper presents some initial findings.

2. Observation Plan

The target selection and observation configurations were designed to address as many of the above questions as possible.

2.1 Target Selection

The third and final observation plan called for identifying four AB pairs that would test the independent variables of separation and position angle. The pairs would need to be sufficiently high in the sky during the winter of 2017 and 2018 to enable both high and low airmass observations within the same night. Predictable targets were selected to be "truth" from the WDS catalogs. After initial test runs of 10 candidates, three were selected from the Catalog of Rectilinear Elements and one from the Sixth Orbital Catalog (Table1).

Target Star Selection		
Magnitude	Separation of A to B	
Difference	6" - 10"	10" - 15"
0 to 1.99	J 703	STF 911
	07106+1543	06269+0404
2.00 to 5.00	STI 579	POU 1245
	05446+6320	06214+2431

Table 1. Target stars by separation and magnitude difference.

The predicted separation and position angles for each of these targets were calculated as depicted in Table 2 under "ephemeris 1/1/2018". The observations were performed from late November 2017 through early March, 2018. The January 1, 2018 was chosen as being near the midpoint of the observation period. Note the large error for the two rectilinear solutions for STI 579.

Double Star Characteristics					
Star Parameters	**J703**	**STF 911**	**STI 579**		**POU 1245**
WDS Number	07106+1543	06269+0404	05446+6320		06214+2431
First Observation	1912	1829	1908		1892
Last Observation	2012	2017	2016		2010
Magnitude of A	10.43	8.65	10.9		8.77
Magnitude of B	12.4	9.04	13.3		11.1
Magnitude Difference	1.97	0.39	2.4		2.33
Separation - last	10.4"	11.7"	8.4"		14.1"
Solution	6th Orbital	rectilinear	rectilinear	rectilinear	rectilinear
Reference	Cve2008d	Hrt2017a	HRT2017a	USN2013a	Hrt2017a
Ephemeris 1/1/2018:					
separation (rho)	10.059	11.66	7.99	7.88	14.05
error		0.14	2.87	1.55	0.59
position angle (theta)	112.8	155.44	121.72	122.60	19.58
error		0.46	16.00	12.96	2.88

Table 2. Target stars data and predicted rho and theta at January 1, 2018

The researchers used multiple filters in our initial plans. Due to the large number of variables being investigated in the final plan, the team reduced the tested filters to green and red. For the 0.4m SRO telescope the researchers patured10 images for each filter and exposure configuration. For the other telescopes the tam took five of each. Short and long exposures (e.g. 15 seconds and 30 seconds) were taken depending on the optical train and star magnitudes.

Observations were scheduled beginning in late November, 2017. Due to weather, robotic scheduling system constraints, and failed attempts to take high and low airmass images on the same night with each telescope, the final observation runs were not completed until early March, 2018. The resulting observation runs created an incomplete matrix of all possible observations. Regardless of the incomplete data sets, the single telescope factors could be investigated on several different telescopes and optical trains. By incorporating the LCO and iTelescope networks, the multiple telescope factors could be investigated. The data reduction question was then measured from one LCO data set for one of the double stars, STF911.

Observations were organized by “data set”, the set of images for a single continuous observation run. In total there are 222 data sets from the actual observations.

2.2 Observatories and Equipment

The telescope located at SRO could be dedicated to the project and controlled by BRIEF. Eight iTelescope systems were initially planned to be used but the two smaller systems (a 90mm and a 106mm) proved to be inadequate for the measurements. The iTelescope systems are accessed over the internet and have policy restrictions such as only allowing one observation run per night for a customer on any one telescope. This constraint eliminated their use to measure the impact of airmass during an evening on one telescope. The LCO systems are controlled by an automated scheduling system that allocates observations to telescopes based on their availability. Thus the researchers could not control which of the LCO 0.4m telescopes would be used for a single requested observation or the exact timing of an observation. Tables 3, 4 and 5 list the locations, telescopes and CCD cameras that were used for the investigation.

Locations					
Location	Group	Location	Latitude	Longitude	Elevation
#1	ITELESCOPE	Mayhill, NM	32° 54' 13.00" North	105° 31' 42.00" West	2225m
#2	ITELESCOPE	Siding Springs, AU	31° 16' 24.00" South	149° 3' 51.70" East	1165m
#3	ITELESCOPE	Nerpio, Spain	38° 9' 56.00" North	2° 19' 34.80" West	1650m
#4	SRO(private)	Auberry, California	37° 4' 13.00" North	119° 24' 46.00" West	1405m
kb27	LCO	Maui, Hawaii	20° 42′ 27″ North	156° 15′ 21.6″ West	3055m
kb97	LCO	Siding Springs, AU	31° 16' 23.88" South	149° 4′ 15.6″ East	1116m
kb99	LCO	Tenerife, Spain	28° 18′ 00″ North	16° 30′ 35″ West	2330m
kb82	LCO	Maui, Hawaii	20° 42′ 27″ North	156° 15′ 21.6″ West	3055m
kb80	LCO	Texas, USA	30° 40′ 12″ North	104° 1′ 12″ West	2070m
kb26	LCO	Region IV, Chile	30° 10′ 2.64″ South	70° 48′ 17.28″ West	2198m

Table 3. The thirteen telescopes used and their locations.

Telescopes					
Reference	Location	OTA	Aperature	Focal Length	F/Ratio
T11	#1	Planewave 20" CDK	510mm	2280mm	f/4.5
T21	#1	Planewave 17" CDK	431mm	1940mm	f/4.5
T17	#2	Planewave 17"CDK	431mm	2912mm	f/6.8
T27	#2	Planewave 27" CDK	700mm	4638mm	f/6.6
T31	#2	Planewave 20" CDK	510mm	2259mm	f/4.4
T18	#3	Planewave 12"CDK	318mm	2541mm	f/7.9
SRO	#4	RCOS 16" Ritchey Chretian	406mm	3540mm	f/8.9
LCO	see table	RCX 400 16"	406mm	3251mm	f/8

Table 4. Telescope characteristics

CCD Cameras				
Scope	CCD	QE	Full Well	Resolution
T11	FLI ProLine PL11002M	51% Peak	~60,000e- ABG	0.81 arc-secs / pixel
T21	FLI-PL6303E	68% Peak	~100,000e- NABG	0.96 arc-secs / pixel
T17	FLI ProLine PL4710	94% Peak	~100,000e- NABG	0.92 arc-secs / pixel
T27	FLI ProLine PL09000	68% Peak	~100,000e- ABG	0.53 arc-secs / pixel
T31	FLI ProLine PL09000	68% Peak	~100,000e- ABG	1.1 arc-secs / pixel
T18	KAF-6303E	68% Peak	~100,000 NABG	0.73 arc-secs / pixel
SRO	SBIG STL11000M	50% Peak	~50,000 NABG	0.51 arcsec/pixels
LCO all 6	SBIG 6303	68% Peak	~100,000 NABG	0.73 arc-secs / pixel 2X2 binning

Table 5. CCD camera characteristics

2.3 Data Reduction Methods

All images regardless of telescope were processed using Dr. Michael Fitzgerald's OSS Pipeline (Fitzgerald, 2018) to limit uncontrolled variables. The OSS Pipeline acts as an image-processing tool, accomplishing a number of modifications to each image to help ensure accurate measurements. For example, through this tool, any compression of the fits file is removed. To make images more measureable and less susceptible to background noise, cosmic ray traces are removed as effectively as possible, pixels below a certain threshold are removed, and any bad pixels are interpolated using a Gaussian Kernel. The OSS Pipeline provides entirely new WCS coordinates for each image file using Astrometry.net, and any old WCS coordinates were replaced with these new WCS coordinates. The OSS Pipeline also creates new, more readable file names for each image, allowing for easier accessibility and greater efficiency. Though the OSS Pipeline creates six photometry files for each image, these files were not used for the purposes of this study. These photometry files will likely be used in future projects.

For all data sets, all images were measured for separation and position angle using Mira Pro x64. Excel was used to calculate standard deviations and standard error of the mean for all data sets. The same server, Boyce Astro Research Computer (BARC), was used for all files and analysis. For assessing the possible impact of the data reduction tools, the same LCO STF 911 data set was also reduced using SAOImage DS9 (DS9) and AstroImageJ to compare with the Mira Pro x64 reduced data.

The software program Mira Pro 64x was used to measure each image, regardless of telescope. In Mira Pro x64, experienced students measured each image separately. After the image was placed into the program, the vertical transfer function was edited to create a clearer image. A vector was then created between the primary star and the secondary star, with the centroid function set to measure a 5 pixel sample radius. The centroid sample radius was lowered if the image could not be measured with this default centroid. With the vector placed, Mira Pro x64 then calculated the given theta and rho of the binary star system based on the image. In some cases, an image's degree of saturation was measured using Mira Pro x64. This was accomplished by creating a 3D graph of each binary star system that showed the ADU value of each pixel, and any pixel that was found to be above a certain ADU value (the value varied for each telescope) was found to be oversaturated.

The image analysis software SAOImage DS9 was used to measure the position angle and separation distance for each image by placing a 4" circle around the rough center of both the primary and secondary stars using the Regions feature. DS9's auto-centroiding feature calculates the weighted mean position of all counts per pixel enclosed the star, moving the circle's center to the centroid of the star. The coordinates for the centroid of each star were then recorded and placed as the endpoints of a line segment. The length of the line segment provided the separation distance in arcseconds and its orientation provided the position angle.

AstroImageJ for Double Star processing first requires establishing the WCS coordinates in each FITS file, which was provided by the OSS Pipeline using Astrometry.net. When measuring it is essential to reduce the aperture of the AIJ selection tool to a low enough value that the aperture of one star does not conflict with aperture of the other. If this happens, the measurement line connecting the two star centroids will not be in a position near the star centroid. Unlike other software products, clicking on the star will not auto-locate the star centroid. Instead, once the aperture selection tool is reduced to a size that will fit within the star and not conflict with the other star, you have to approximate the stellar centroid. From there, AIJ will compute the centroid within the aperture you set on the star. Once both stars are selected, AIJ then provides a "Measure Tool" window displaying the theta, rho and a delta magnitude for the two stars. In addition to providing the theta and rho measurements, AIJ ties to the SIMBAD database for any further analysis/research. When there is a connection to the SIMBAD catalog, a right click on the star will open your browser window and display the SIMABAD data.

3. Results

Observations were made at 13 telescopes from November 30, 2017 through March 12, 2018. The measurement data by star are contained in Tables 6, 7, 8, 9, and 10 as Appendices following the References section. Two of the tables are for STI 570 used to compare the observations with the two different orbital

solutions. For any combined analysis, the only one of the two could be used avoid statistical bias. USN2013a data was used over HRT2017a due to its lower predicted error (see Table 2).

Table 11 provides an overview of the scope of the observation program. Seven hundred readable images were used from 126 observation runs ("detail observation sets"). Data was combined by star and observation run into data sets for comparative analysis. The lowest level of these is the detail observation sets which are all the images for a filter and an exposure for one observation run – commonly 5 images. Stacked images were created by the OSS Pipeline for some observation runs. The Composite Sets include all the images from a run regardless of exposure as described in their title.

Detail Observation Sets		Images
Green	63	353
Red	57	331
Infrared	6	16
Total Sets	126	700
Stacked Observations		
Green Stack	7	7
Red Stack	8	8
	15	15
Composite Sets of the Images		
ALL	10	184
ALL HIGH	9	351
ALL LOW	8	165
ALL GREEN	27	353
ALL RED	25	331
ALL INFRARED	2	8
	81	1392

Table 11. Types and number of data sets and the number of images used in each type

The Results Tables 6 through 10 group the individual observations into the data sets used for the analysis.

4. Analysis and Discussion

There are many permutations and combinations to consider in analyzing the data. This investigation is limited to analysis the basic statistics for the data sets applicable to the introductory questions listed above. For each data set the standard deviation, error from the predicted separation and position angle, and standard error of the mean is calculated and presented in the Results Tables 6 through 10. These data sets were used to address the questions listed in Section 1.

There were two “outlier” sets of observation that needed attention:

The star J703 is an unusual outlier. Due to its consistent error and small SEM, follow up observations were performed on other telescopes. The initial analysis of those additional observations are consistent with the ones in Table 6. At this time it appears that the ephemeris for the orbital solution may be in error thus causing significant and consistent error from the “truth”. Though this warrants further research, that is outside the scope of this investigation. Except as noted in the following analysis sections, the data for J703 are not included in the analyses for mean error.

The observations from iTelescope T17 show consistently high mean error and SEM throughout the analyses and are noted in many of the figures. These data were left all the analyses to show the effects of an outlier on the broader statistics.

4.1 Filters and Saturation

Figures 1 and 2 display the mean errors from the “truth” for all of the 126 detail observation sets and their and their standard errors of the mean (SEM). Exposures ranged from 15 seconds to 60 seconds, which causes varying degrees of saturation. Each of the detail data sets were characterized as unsaturated, partly saturated, and saturated. Nearly all of the outliers were unsaturated. Several of these outliers (e.g. iTelescope T17 on March 12, 2018) also are outliers in other analyses further in this paper.

These figures suggest that saturation may be a less significant factor in measuring double stars than considered in the past. Secondly, the consistently large SEM for the SRO telescope suggests that some form of calibration may be warranted for that system. Such a calibration procedure may be a good practice for all systems to establish their potential degree of error and uncertainty. More broadly, it would appear that red filter observations are potential less certain than green.

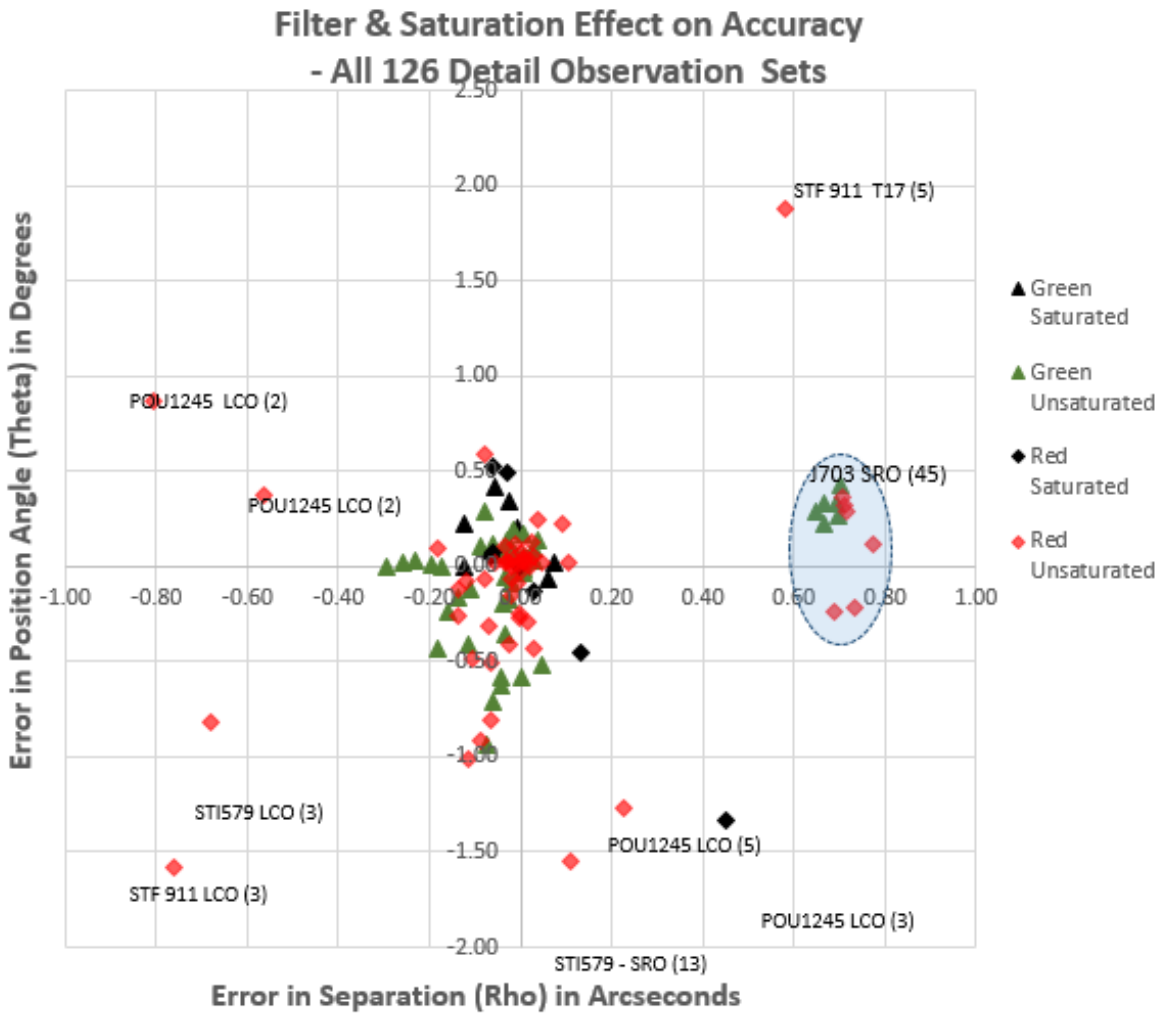

Figure 1. Plot of the mean error in position and *separation for the 126 detail observation sets* measurements coded by saturation and filter

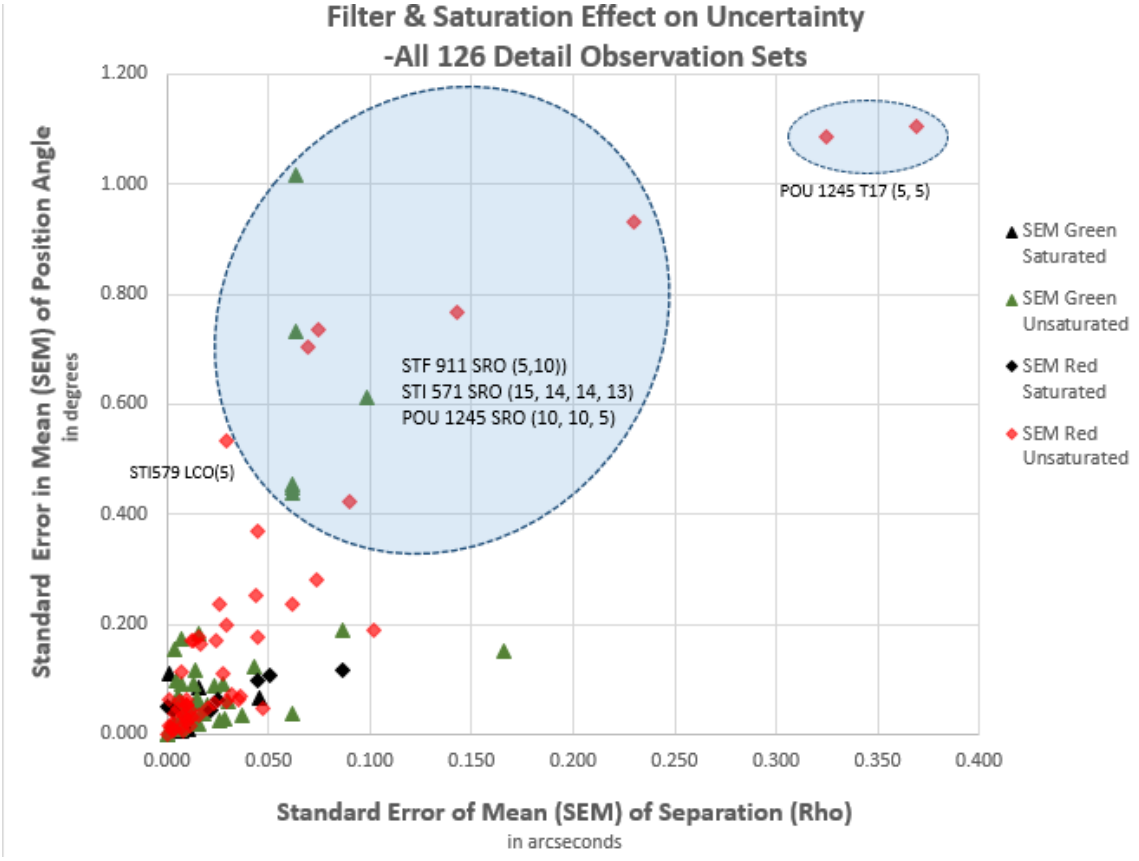

Figure 2. Plot of the standard error of the mean (SEM) in position and separation measurements coded by saturation and filter

The question of CCD image saturation warrants further examination. The automated centroid calculation function is critical in most astrometry software to provide consistent results. Figure 3 is a typical screen grab of a measurement in Mira Pro 64. Looking at the image one could see that there could be some degree of uncertainty in the calculation of the centroids. It would be difficult to do reliably by eye alone.

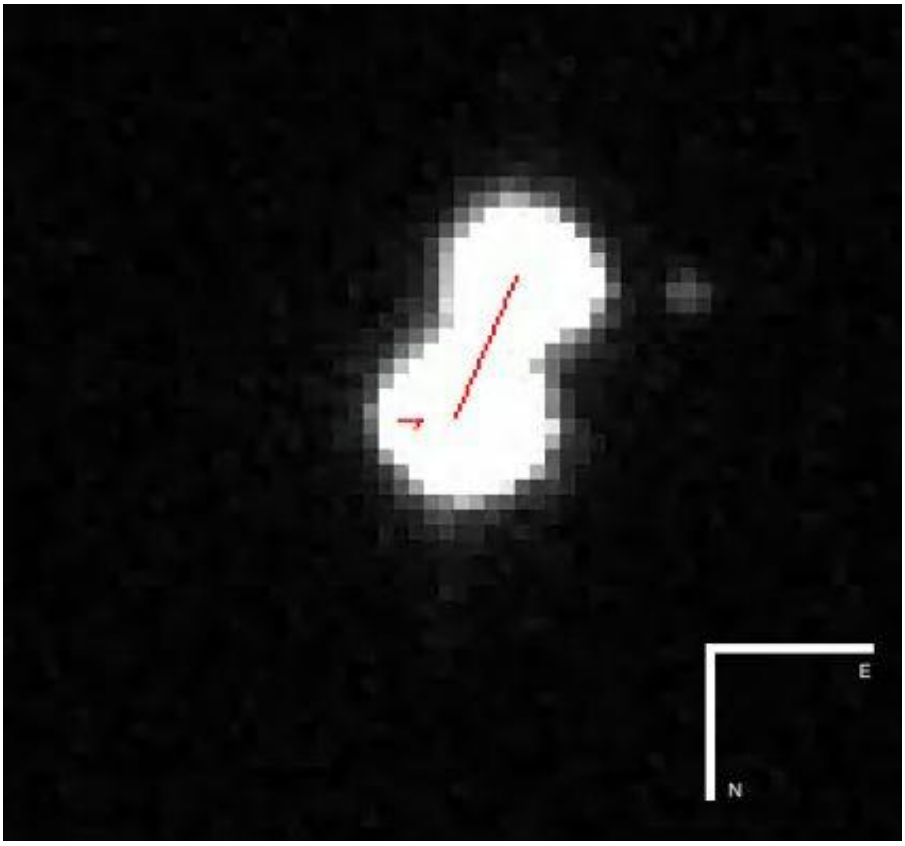

Figure 3. A saturated image taken by the telescope LCO kb97 of the binary star system STF 911

Figure 4 is a wireframe of the same image taken from Mira Pro 64. Note that the peak of the brighter star is above 100,000 ADUs and thus well saturated.

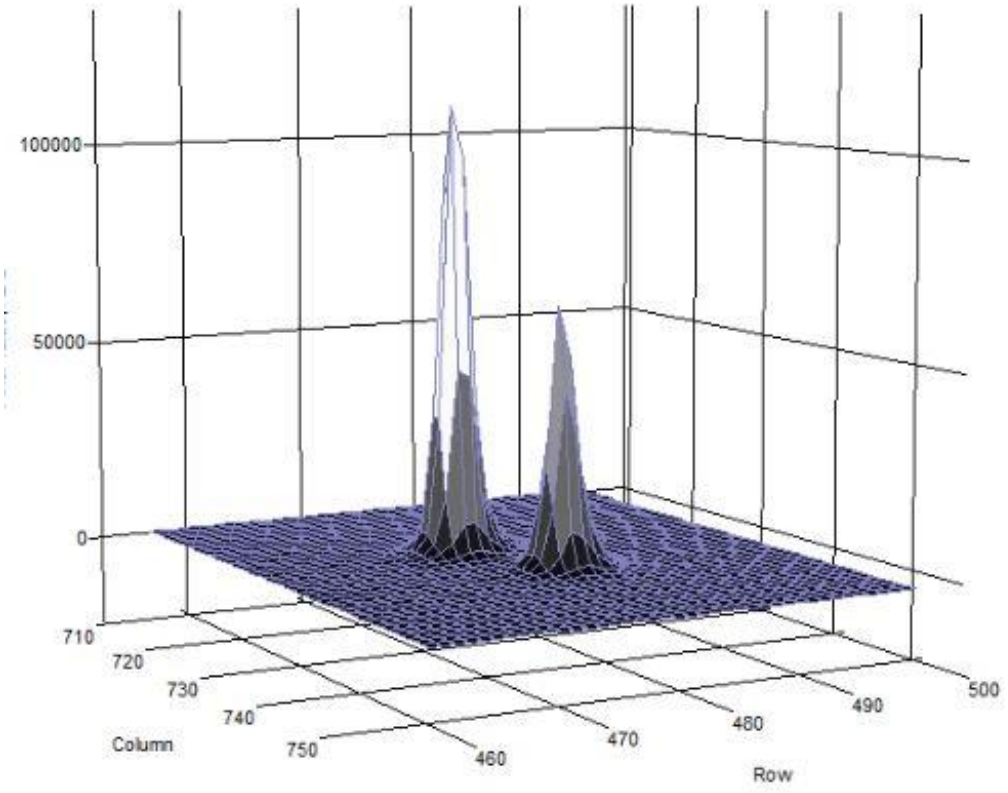

Figure 4. A 3D model of the image in Figure 3 representing the ADU values for each pixel

A vertical view of the saturation of the double star is shown in Figure 5. Note that an area of 3 by 3 pixels is white indicating saturation.

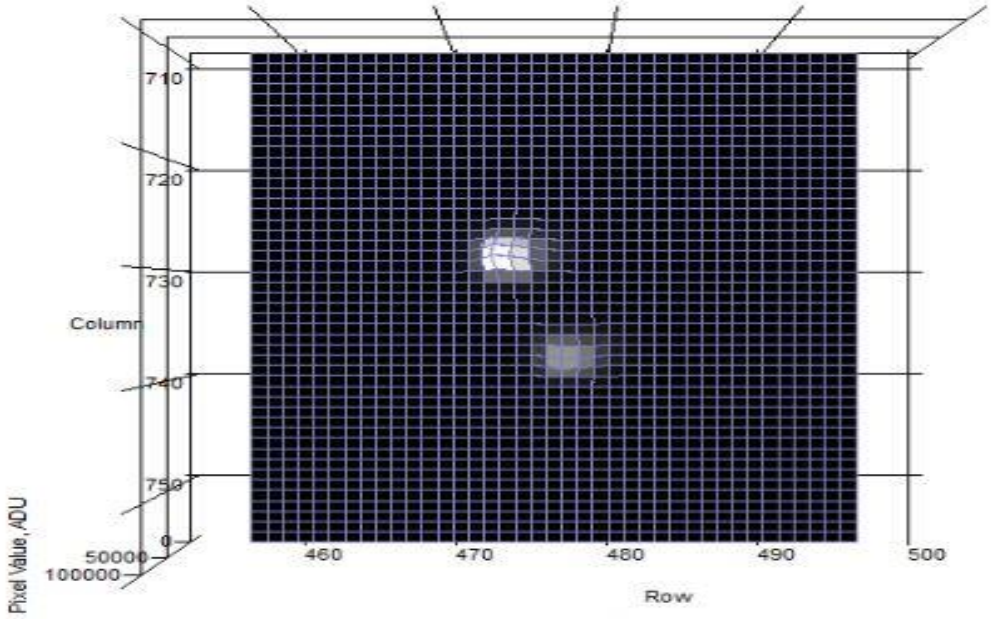

Figure 5. A vertical view of the 3D model in Figure 4

Figures 6, 7, and 8 provide the same views from Mira Pro 64 for a double star with an unsaturated primary image, under 20,000 ADUs. In Figure 8 one can see only bare evidence of the secondary star (~2,000 ADU) though it appears prominent in Figure 6. Possibly such a faint image could lead to the errors seen in Figures 1 and 2 which are exclusively from unsaturated image data sets.

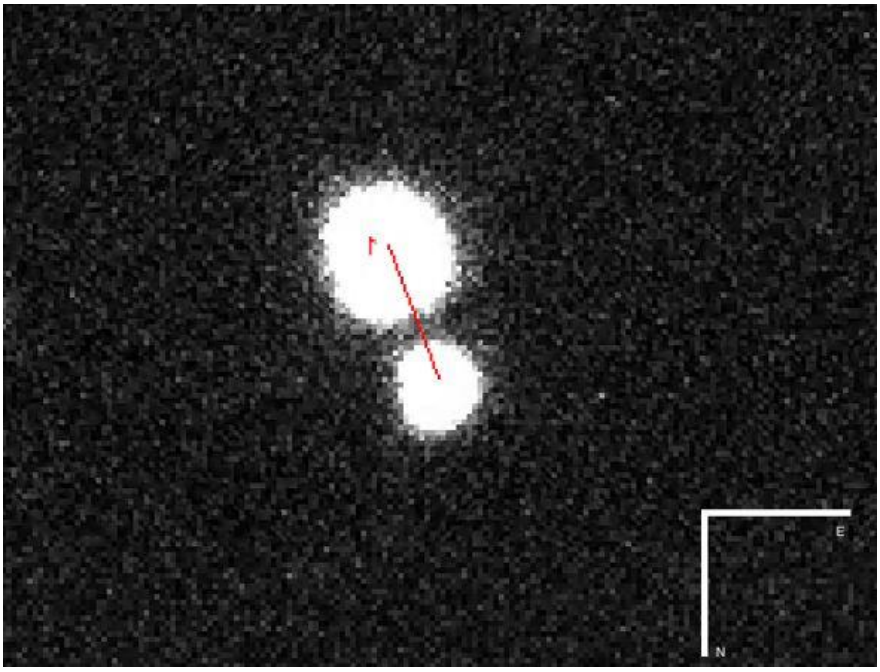

Figure 6. An unsaturated image taken by the SRO telescope of the binary star system POU 1245

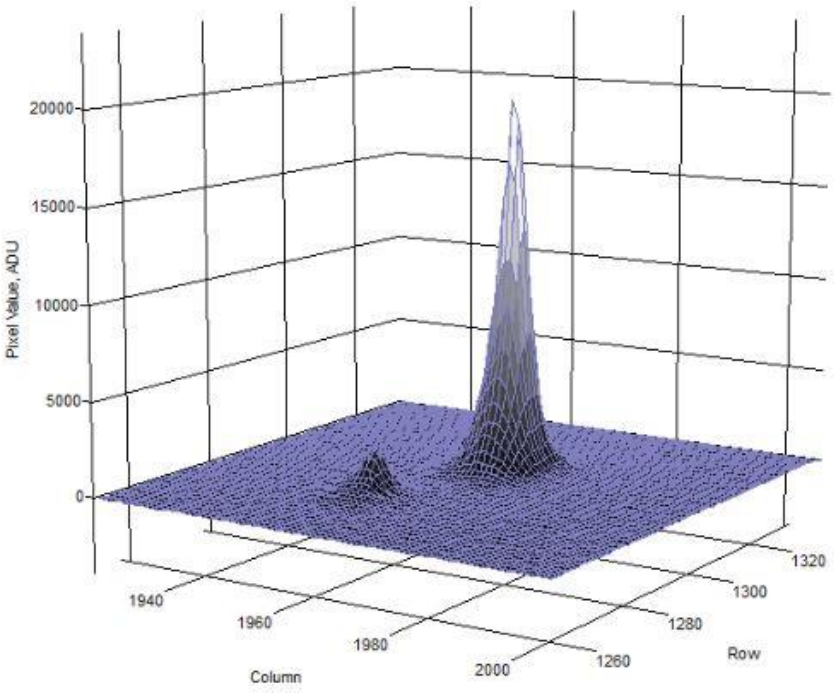

Figure 7. A 3D model of the image in Figure 6 representing the ADU values for each pixel

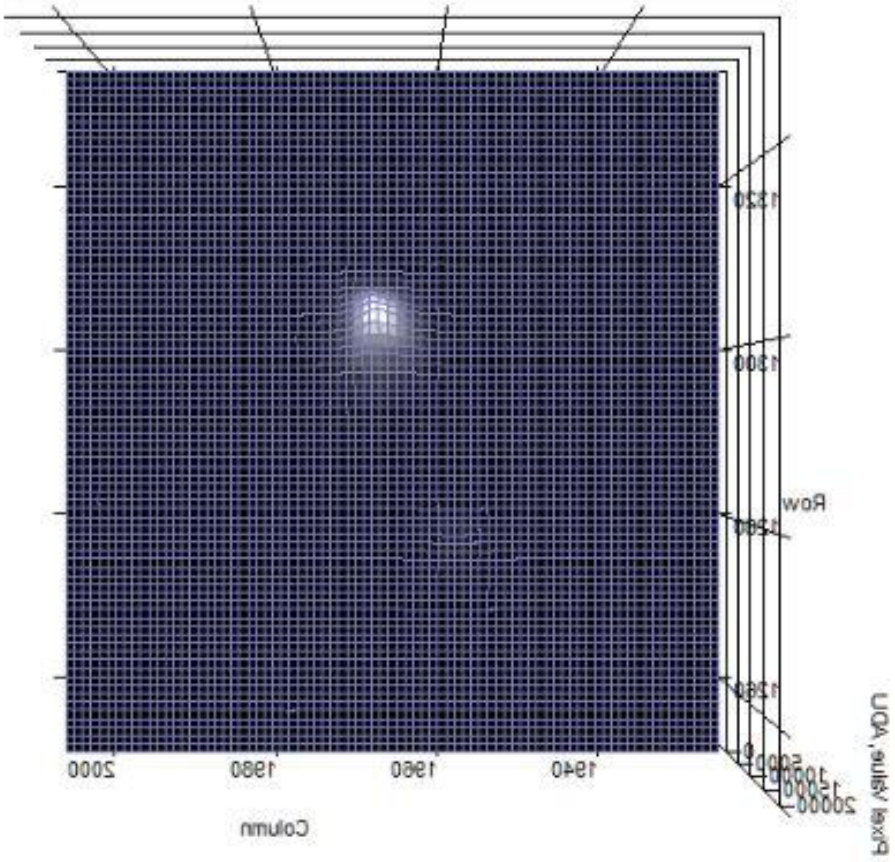

Figure 8. A vertical view of the 3D model in Figure 7

Some of the images and image sets in the observations were extremely saturated. Figure 9 is an example of a "super-saturated" image having two flat tops at ~65,000 ADUs. The fully saturated pixels can be seen in Figure 10 having an area of about 5 X 6 pixels for the primary.

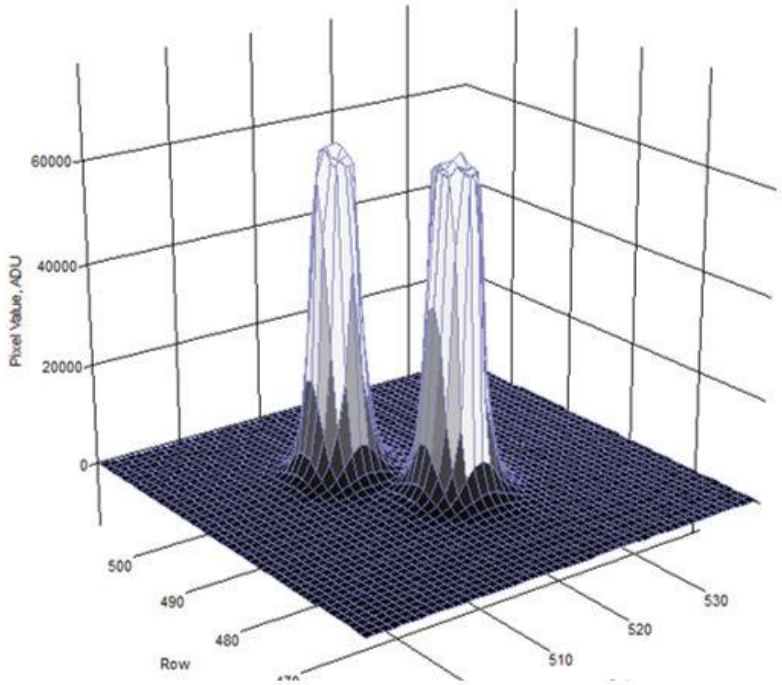

Figure 9. A 3D model of an extremely saturated, or "super-saturated" image

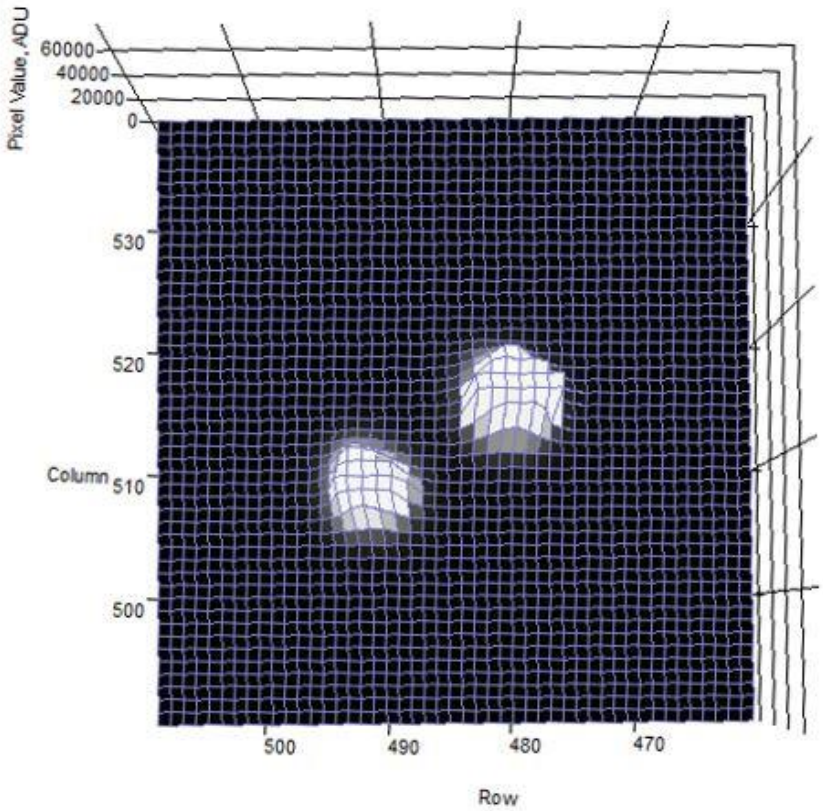

Figure 10. A vertical view of the 3D model in Figure 9

In Figure 11 a 3 pixel radius aperture is placed over the two saturated areas. If the aperture radius is adjusted properly, the saturated areas can be covered to compute a centroid. Variations could occur due to local maxima as may be seen in Figure 9. This may account for the accuracy and relatively small SEM of the saturated images.

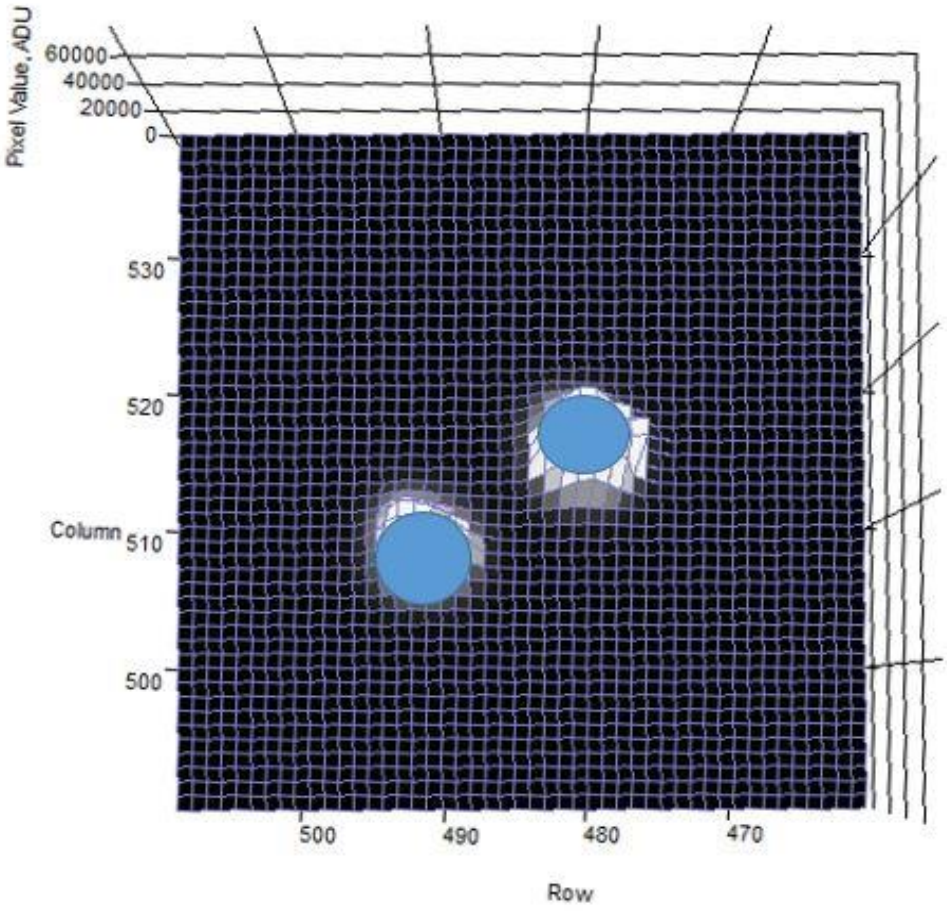

Figure 11. A vertical view of the 3D model in Figure 9, in which 3 pixel radius apertures are placed over saturated areas.

To pursue this further, researchers analyzed the images for STF911 from T17 and T21. These data sets had varying degrees of saturation. The saturated flat top area was calculated for each image and compared to the errors and SEMs for the images. Figure 12 shows that the error is small until the saturated area reaches ~25 pixels. The SEM begins to rise at about an area of ~20 saturated pixels.

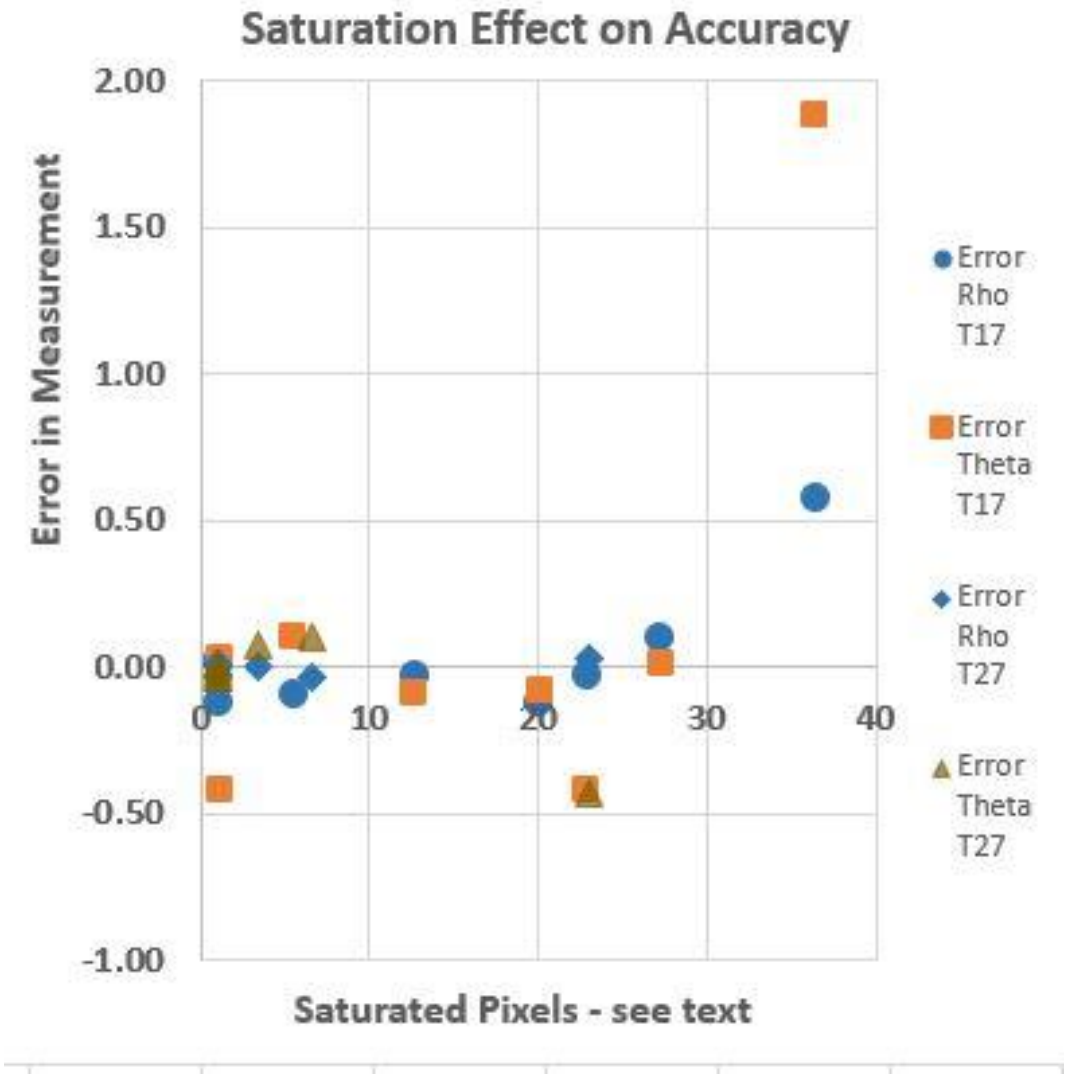

Figure 12. Plot of the mean errors in Rho and Theta for STF911 as a function of the number of saturated pixels for iTelescope's T17 and T27

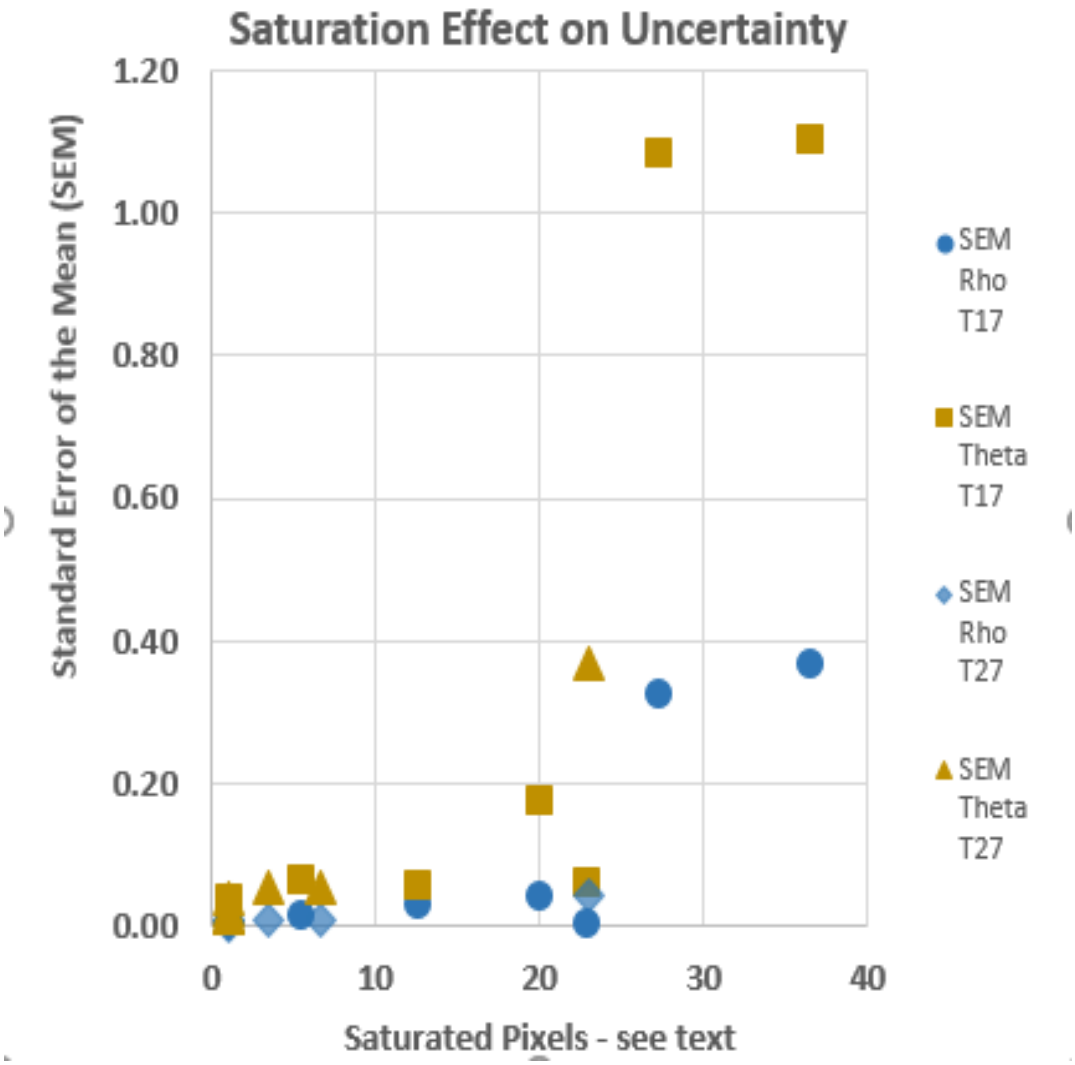

Figure 13. Plot of the standard errors of the mean (SEM) for STF911 in Rho and Theta as a function of the umber of saturated pixels for iTelescope's T17 and T27

Based on this limited data one might surmise that saturation becomes a very significant factor if an image exceeds 20 saturated pixels. Below that threshold would not seem to harm the measurement significantly. Managing the aperture to create a proper centroid would seem to be an important factor in a measurement.

4.2 Separation and Magnitude Difference

Though there are four stars in the investigation, only three could be used for these evaluations. J703 had to be excluded due to its seeming erroneous ephemeris. The remaining three stars had separations of 7.88", 11.66", and 14.05". Over this modest separation range, no clearly discernable trend could be seen. The error in red data in Figure 14 would seem to be greater for the wider pairs. The green data plotted in Figure 15 is actually a bit tighter around the "truth" but it has an odd bias toward negative values (mean error less than "truth").

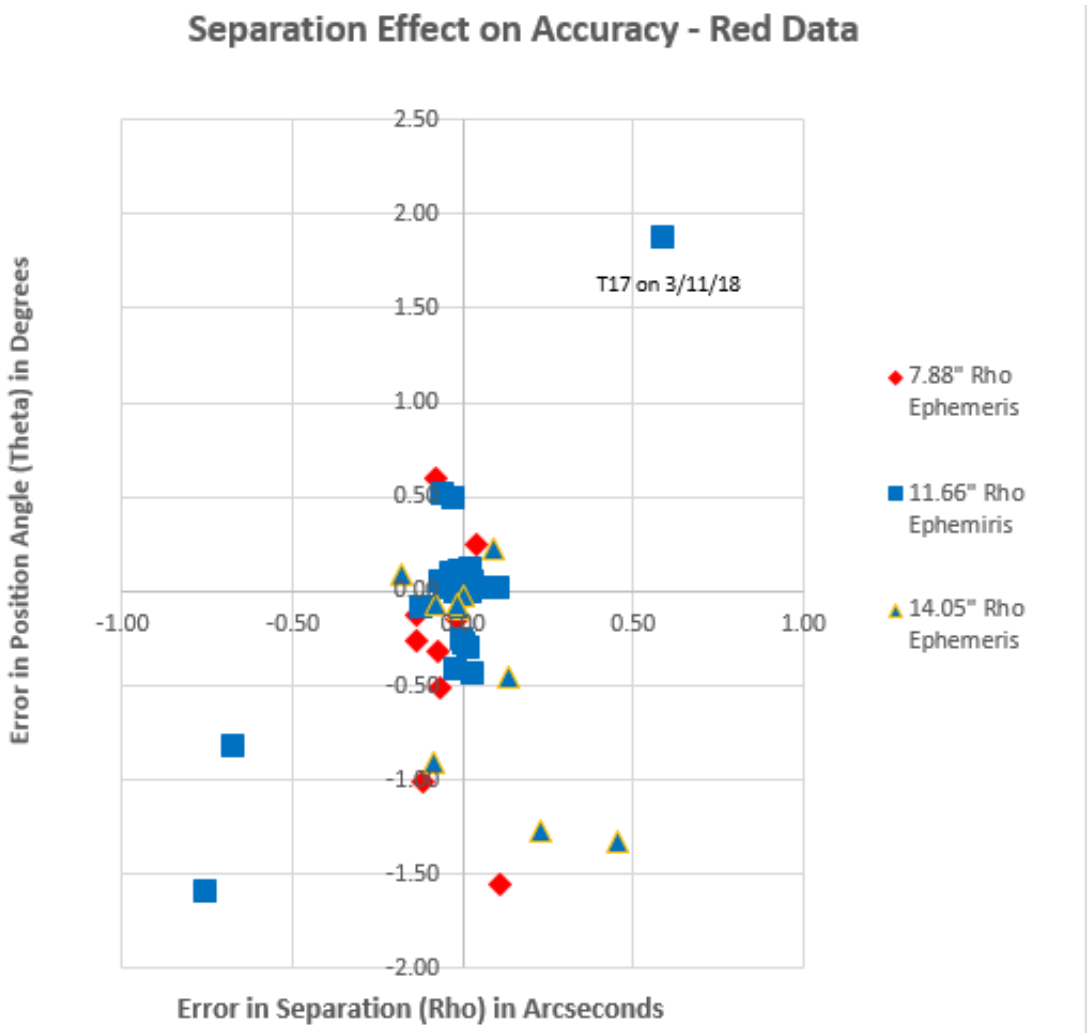

Figure 14. Plot of the impact of separation on the mean error for measurements taken with a red filter

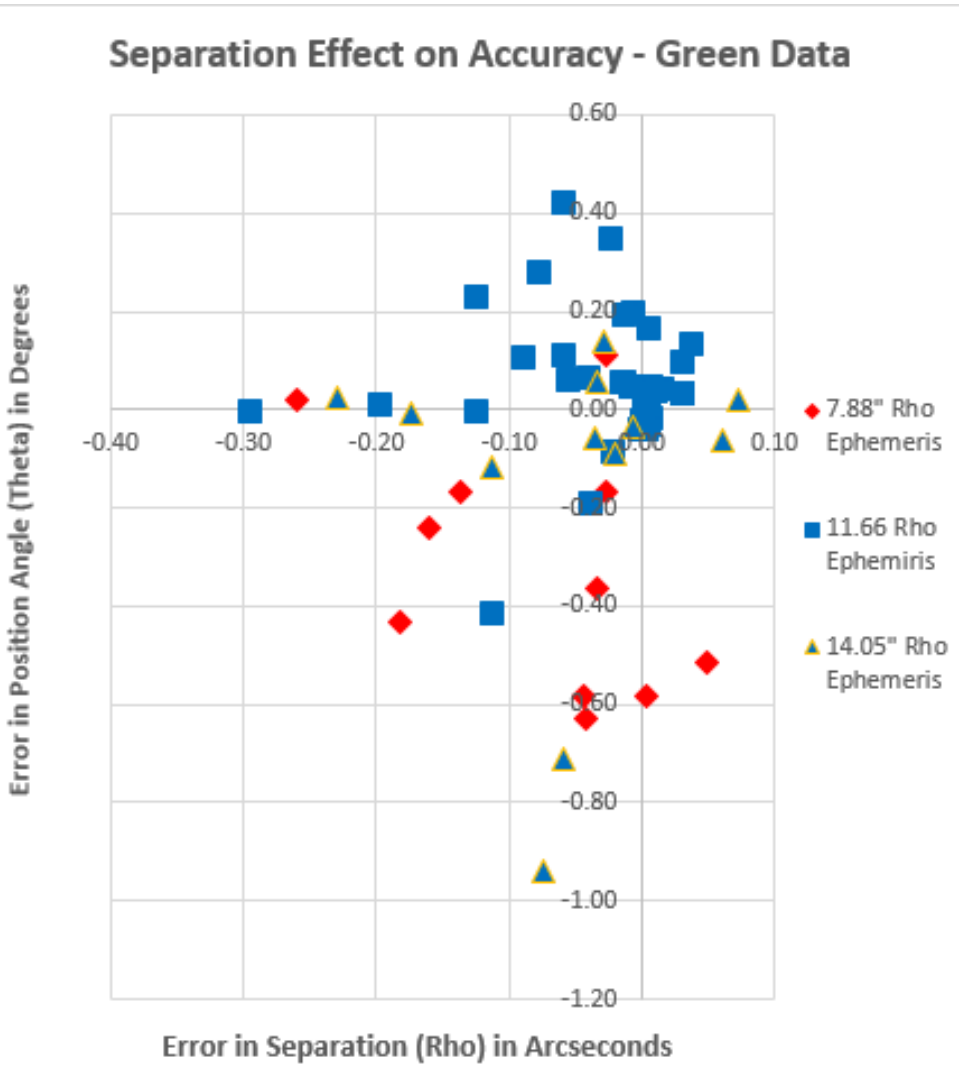

Figure 15. Plot of the impact of separation on the mean error for measurements taken with a green filter

The difference in magnitude between the primary and secondary stars often poses observation problems especially for close pairs. It may be difficult to capture enough photons from the secondary star with a long exposure that causes "blooming" saturation for the primary star. The differences (delta magnitude) in the stars are only 0.39, 2.33, and 2.4 which are not challenging differences at these separations. No discernable pattern was apparent in the data red data (Figure 16) or the green data (Figure 17).

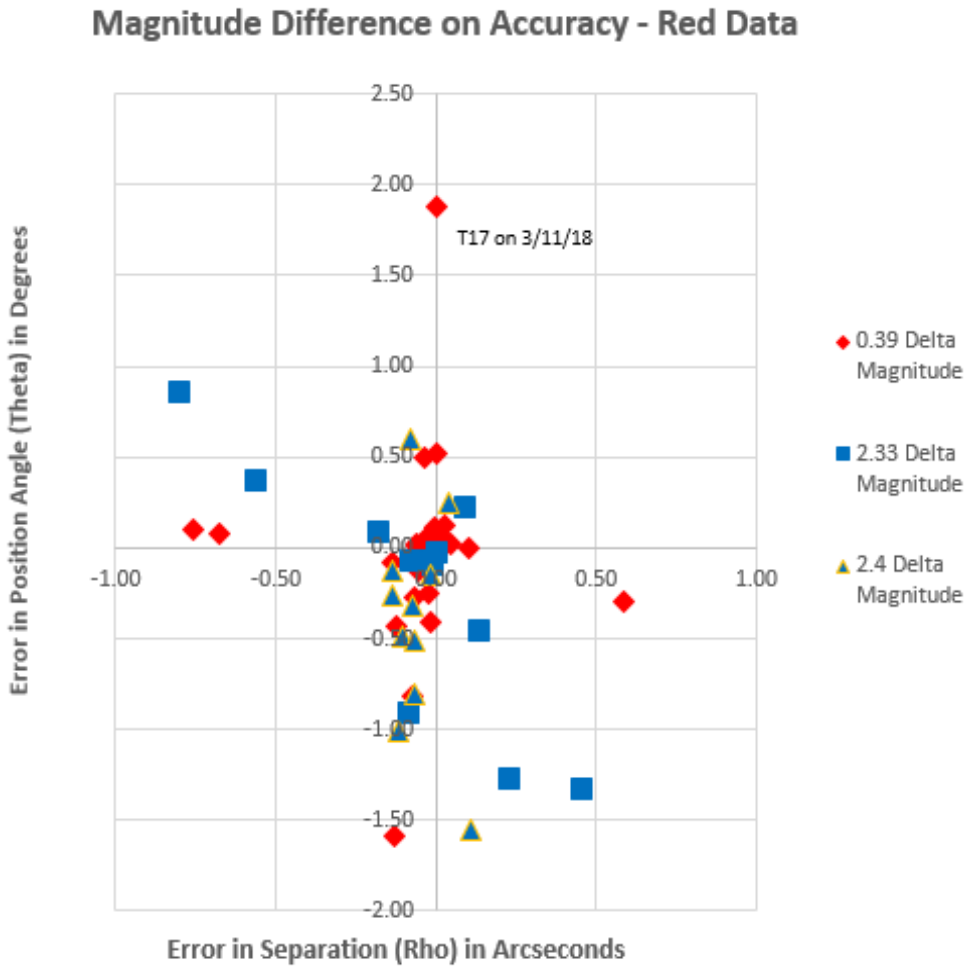

Figure 16. Plot of the impact of magnitude differences on the mean error for measurements taken with a red filter.

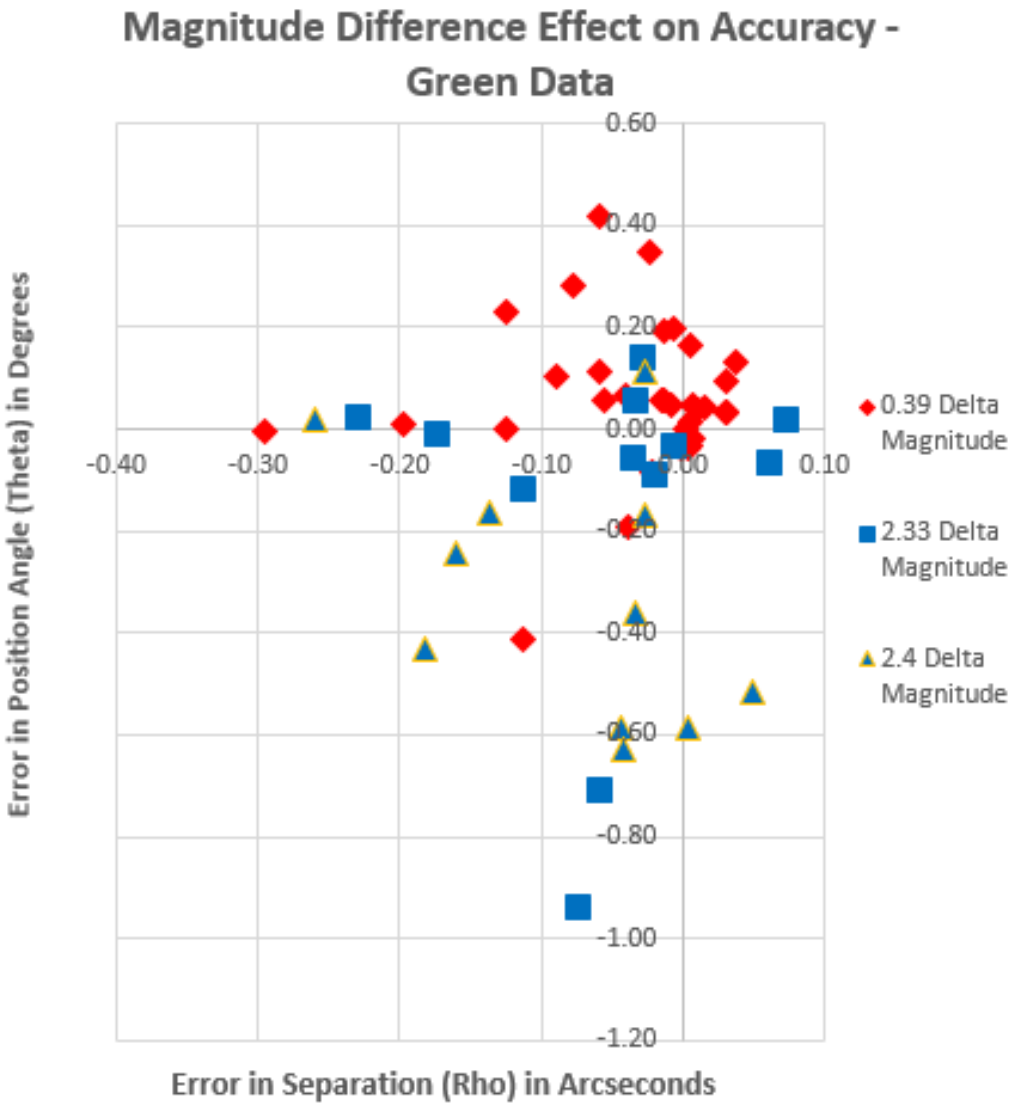

Figure 17. Plot of the impact of magnitude differences on the mean error for measurements taken with a green filter.

4.3 Airmass

Observing near the horizon (e.g. below 30 degrees altitude, about 2X airmass) should introduce more error and uncertainty in the measurement. Only a few data points exhibited this expectation and most showed an indifference to airmass and filter as depicted in Figures 18 and 19.

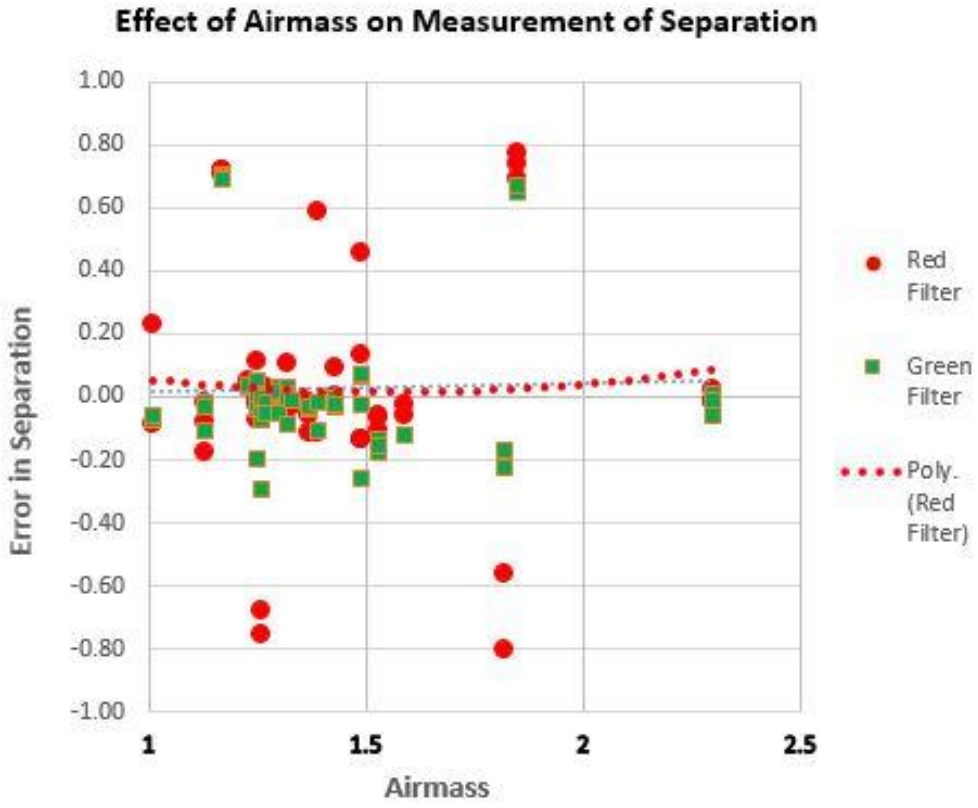

Figure 18. Plot of the mean error in separation by filter as a function of the observation airmass

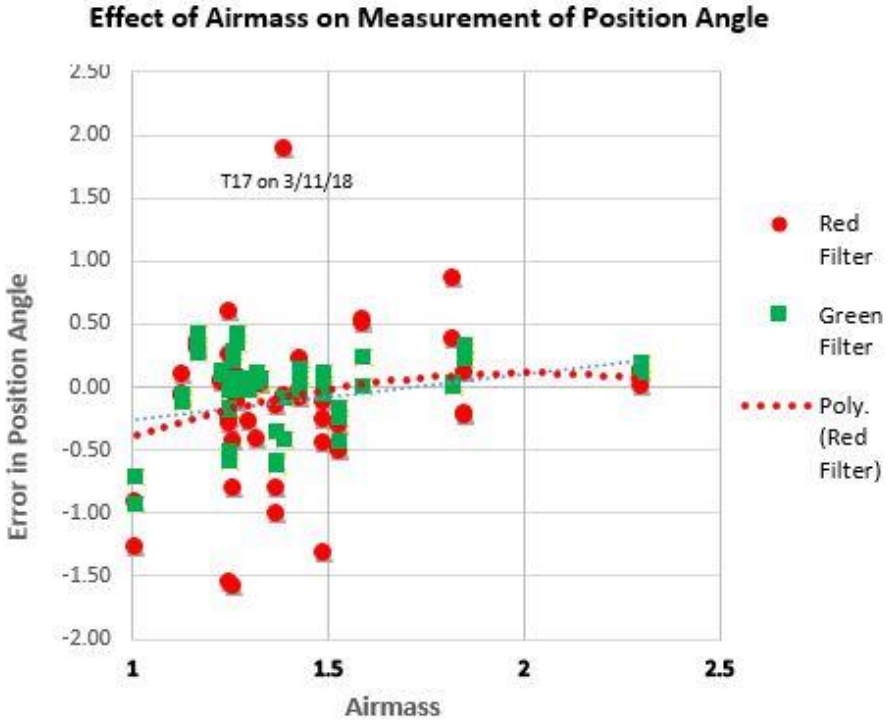

Figure 19. Plot of the mean error in position angle by filter as a function of the observation airmass

4.4 Telescope Aperture

The six iTelescope systems ranging in aperture from 318mm (12.5 inches) to 700mm (27 inches) provide a convenient test bed for this factor. One would expect somewhat less error from the larger telescopes. The data in this investigation is surprisingly indifferent to aperture. In fact the smallest and largest telescopes both displayed essentially the same very small error from the "truth" aside from the two outliers, T17 and T31, in Figure 20.

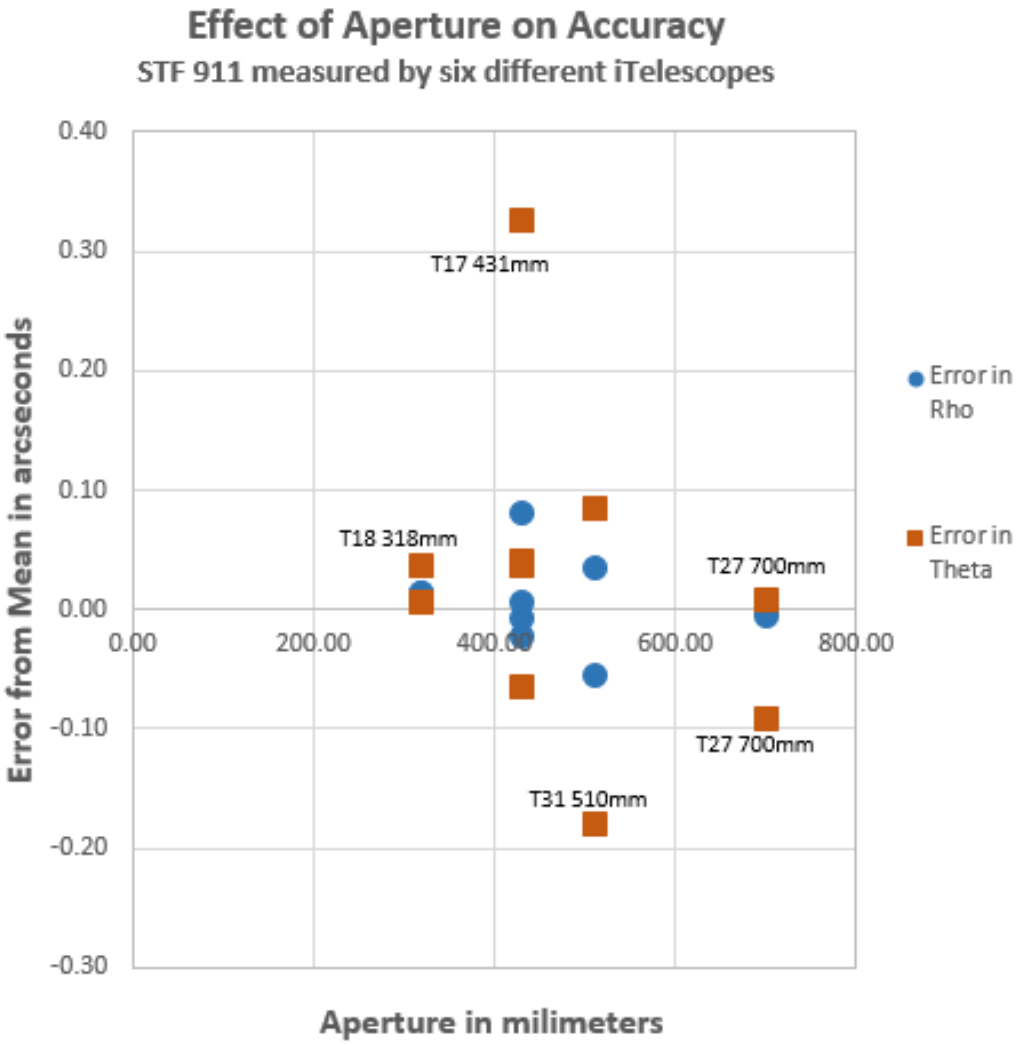

Figure 20. Plot of the mean error in rho and theta as a function of telescope aperture

4.5 Camera Resolution

The six iTelescope systems have varying high quality CCD cameras as outlined in Table 5. To compare their performance the CCD pixels needed to cover an arcsecond of image is a good shorthand measure of resolution that accounts for most of the factors affecting resolution. As with aperture, differences in mean errors were small over this range of (0.53 arcseconds/pixel to 1.1 arcseconds/pixel) except for T17 outlier again as shown in Figure 21.

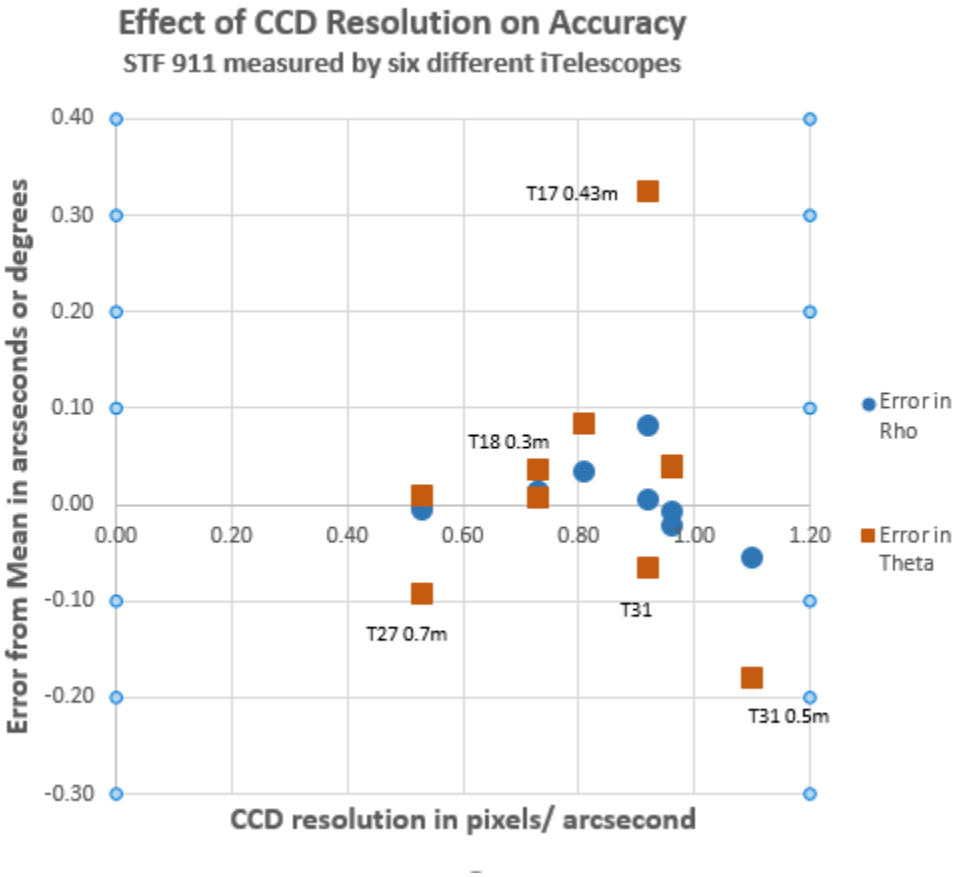

Figure 21. Plot of the mean error in rho and theta as a function of CCD camera resolution measured in pixels/arcsecond

4.6 Averaging Observations

A single measurement of a double star can be readily questioned for accuracy. The question is how many images are needed to make a good observation. The observation data sets in this investigation range in number from one to 15 images using the same configuration of filter and exposure. Figures 22 and 23 provide some insight to the question. The mean error and SEM for the data sets under five images are clearly less desirable

than those of 5 or more. The sets of 5 are well clustered near zero in both mean error and SEM.

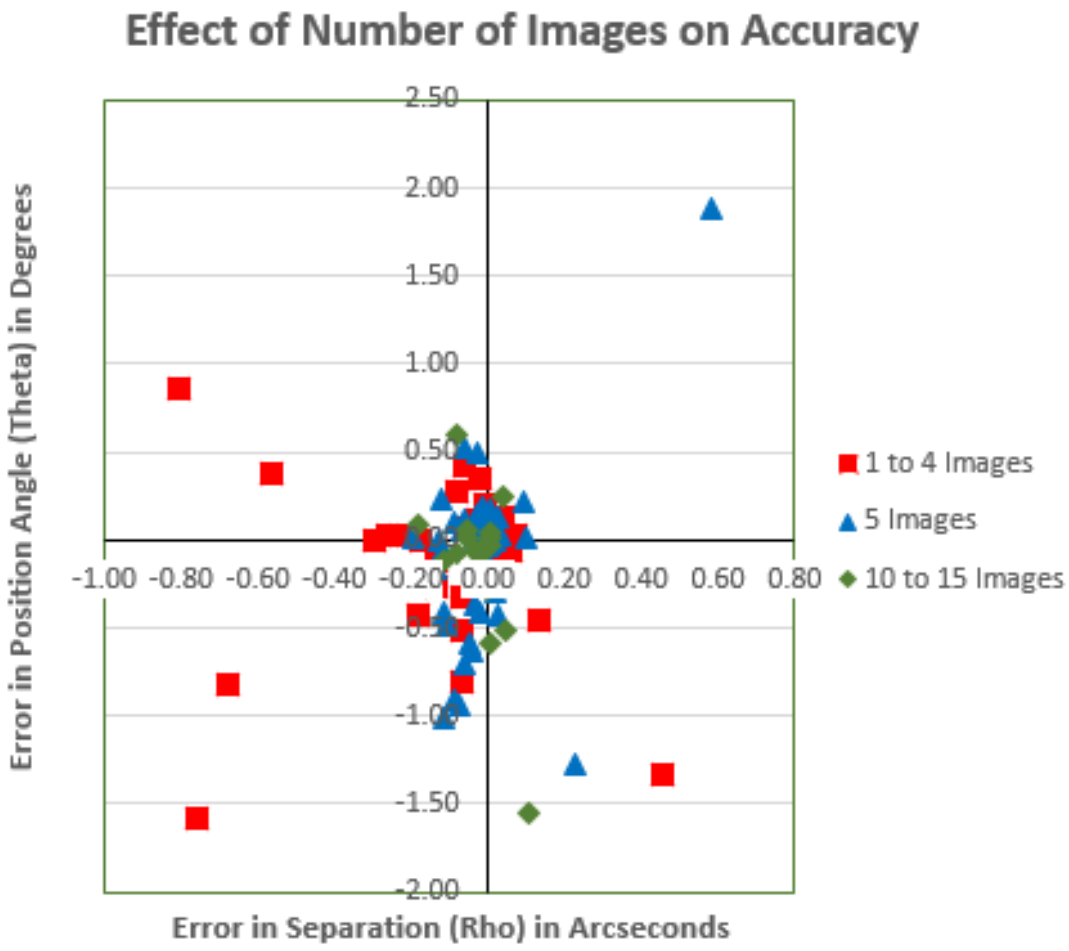

Figure 22. Plot of the mean errors in rho and theta for detail observation data sets of varying numbers of images

SRO was the only system that performed runs of 10 to 15 images. Many of those observation data sets had high SEMs as highlighted in Figure 23 but they show low mean error in Figure 22. As might be expected, the

uncertainties in that system were overcome by increasing the number of images taken.

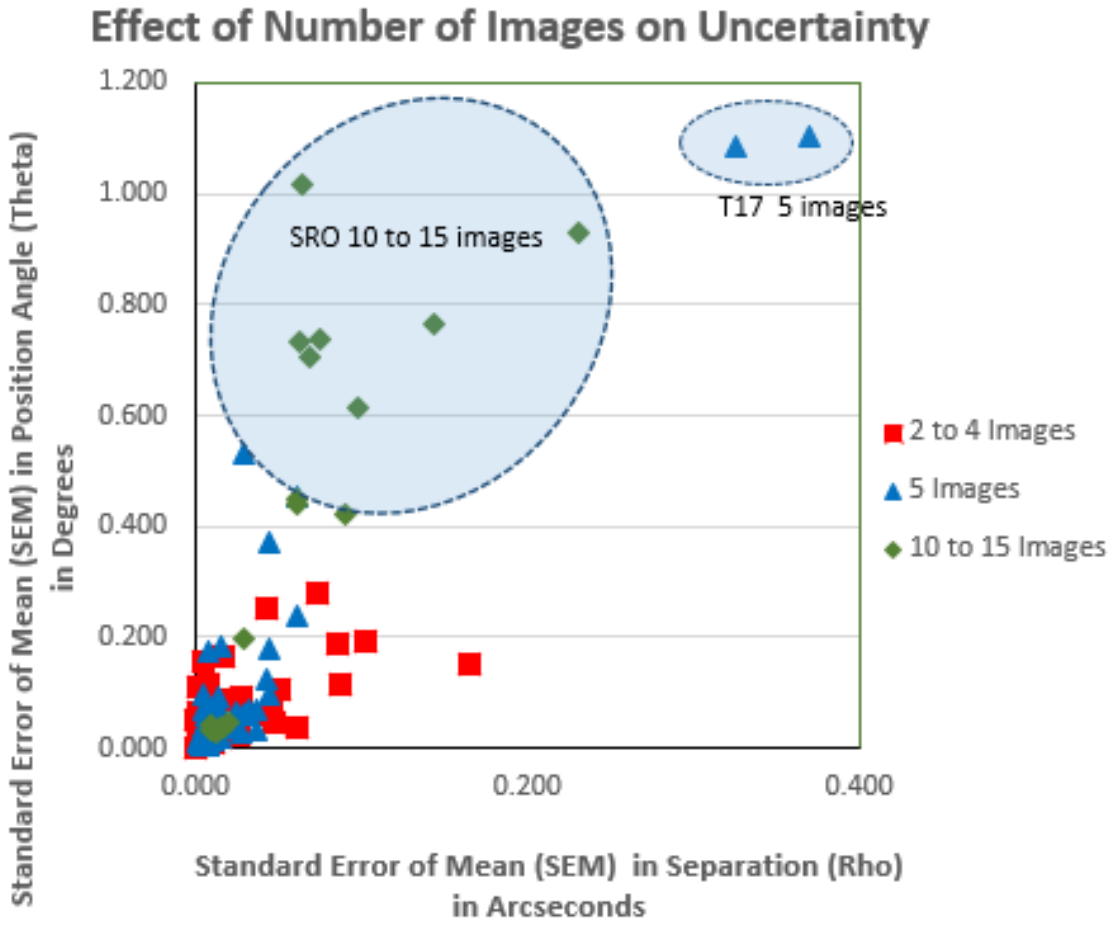

Figure 23. Plot of the standard errors of the mean in rho and theta for detail observation data sets of varying numbers of images

Figure 24 displays the effect on the mean error of averaging varying filters and exposure times for images captured in a single observation run. The "Green Mean" and "Red Mean" are for all exposures of that filter on the observation regardless of their duration. The "All Mean" is the mean of all images captured on one exposure run. The "Stacked Green" and Stacked Red" are stacked images from single observation runs that were created by the OSS Pipeline.

The average SEM for the "All Mean" is 0.006" arcseconds in separation and 0.020" degrees in position angle. For the "Green Mean" they were 0.026" and 0.005" respectively. The "All Red" the average SEM was 0.017" and 0.050" respectively. The "All Mean" had more images per set and that accounts for only some of its better SEM. Averaging all images together regardless of exposure or filter seems to decrease error in the

observations made in this investigation.

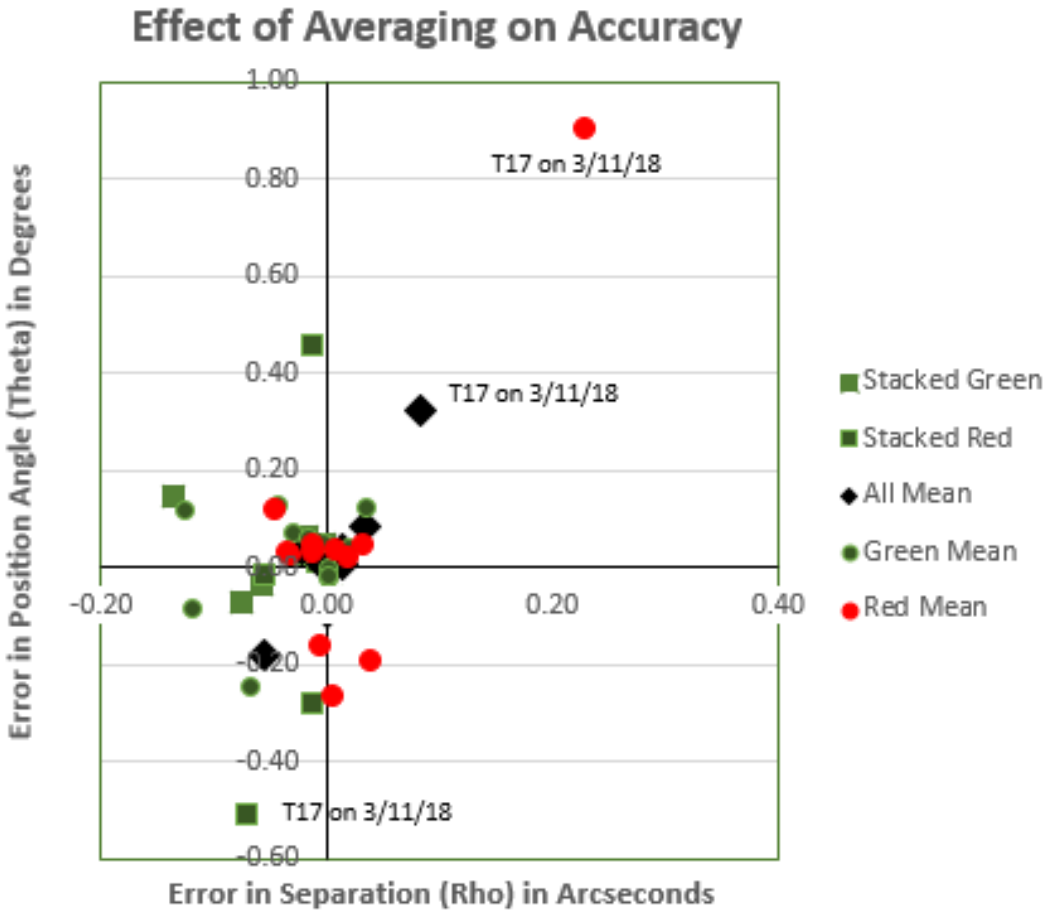

Figure 24. Plot of the mean errors in rho and theta for composite data sets and stacked images

The averaging did not resolve the problems with mean errors for the T17 observations but it largely did for the other observation runs. Refer to Figure 1 for a comparison. So is there a way to identify a bad run from its

statistics and disregard its results?

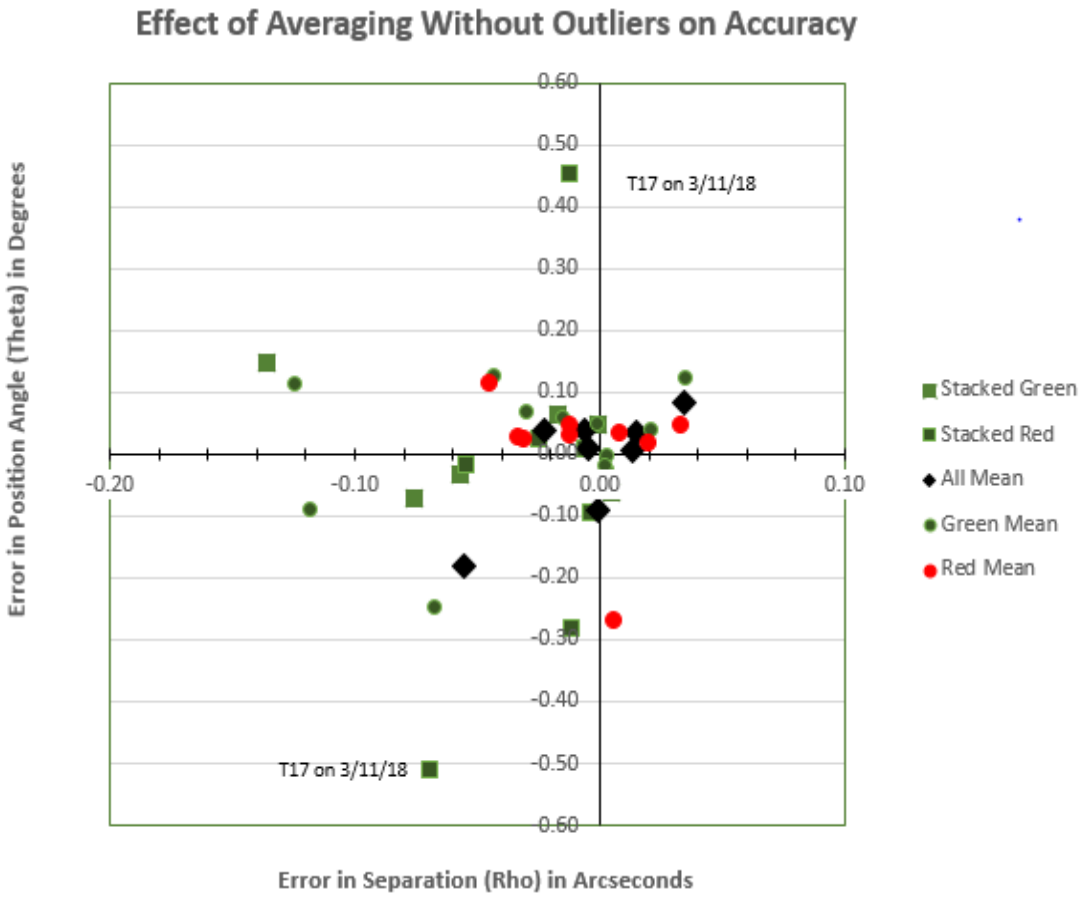

Figure 25. Plot of the mean errors in rho and theta for composite data sets and stacked images after removing any data set with a SEM of more than 0.15" in rho or 0.15 degrees in theta

By arbitrarily rejecting any observation set with a SEM of greater than 0.15" in separation or 0.15 degrees in position angle, the T17 mean error outliers are removed from the results as shown in Figure 25. Over 75% of the remaining averaged data fall within 0.10" of the "truth" in separation and 0.1 degrees in position angle. Thus a maximum SEM criteria may be useful to avoid reporting erroneous measurements. Note that the Stacked Green and Stacked Red data are single images without a SEM. This lack of statistical measure may be a strong reason to avoid using stacked images; their accuracy cannot be predicted.

On four occasions, the same observation run was performed on successive nights with the same iTelescope. Figure 26 displays these results as barbells with the black diamond representing the "truth" for STF911. If one considered the midpoint of each barbell as being the average of the two successive nights, it is clear that one night's observation will be closer to the truth than the second night's observation. The midpoint (approximate mean) of each of these barbells is further from truth than the better observation and better than the worse observation. If only one of the observations were made, one would not know if that one is the better or the worse observation. Also doing a second night observation can provide a warning about an outlier. If the first night's observation gave consistent data like the T17 one in the figure in the upper right, one would not necessarily know about its error without the second night's observation. Averaging two nights may not improve accuracy but it should improve certainty.

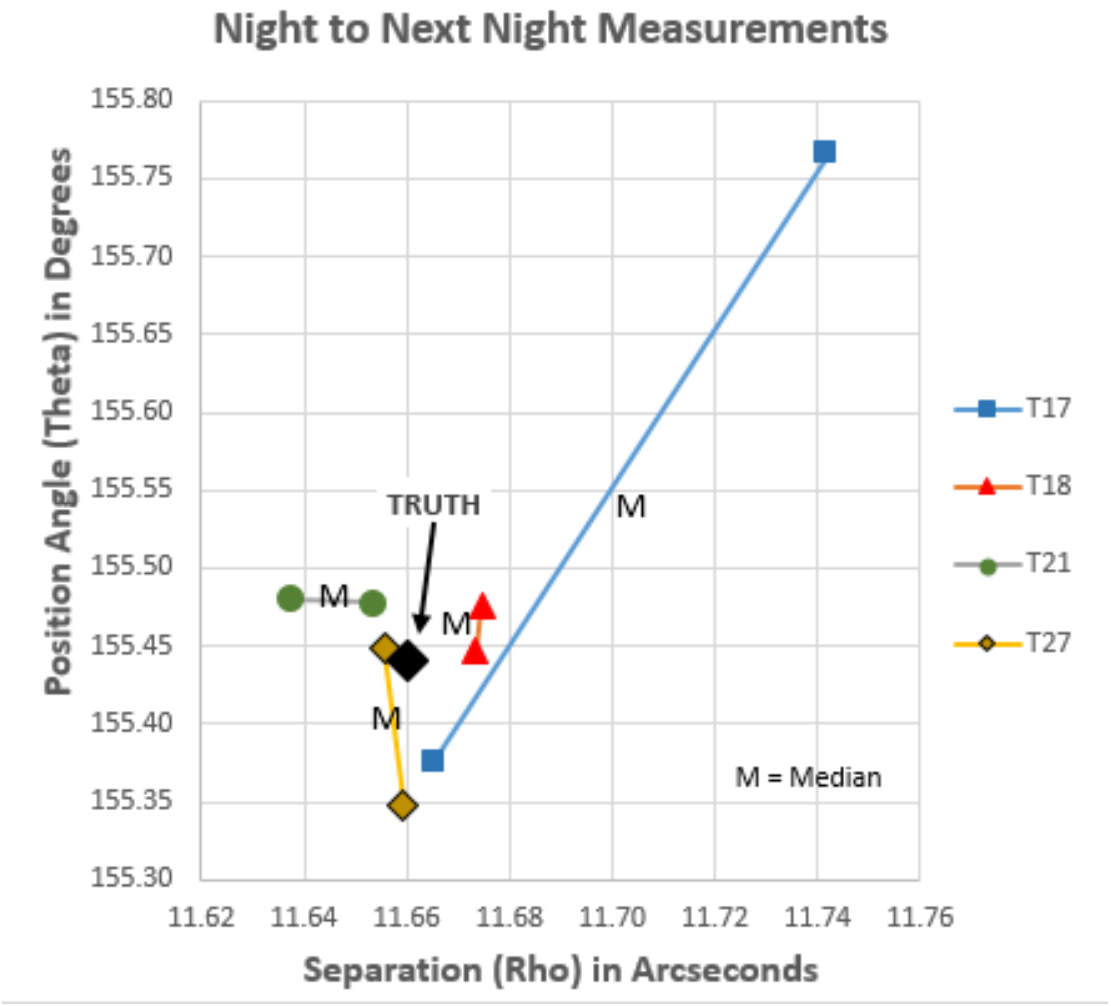

Figure 26. Plot of the mean errors in rho and theta for identical observation runs of STF911 that were performed on successive nights from four iTelescopes

Students often ask how many nights apart observations could be made to be still be included as one observation. This depends on many factors beyond the scope of this investigation. The data from this investigation may help in determining an answer if future investigations are performed.

With the availability of worldwide robotic telescopes, one may ask whether observations from different systems and/or locations be averaged together. The LCO network provides a unique opportunity to attempt to address this. All the LCO systems available to the team are identical 0.4m telescopes with identical cameras at six different locations throughout the world. Observations were made of three of the stars each using three of the identical systems. The observations were not simultaneous and were days to weeks apart. Figures 27, 28 and 29 provide those results and Tables 7 through 10 in the Appendix provide the details.

In each figure the ALL MEAN data is plotted for each observation run. The mean of all measurements is also plotted as an X. As discussed earlier these broad averages can provide most certain data. The ‘truth” is shown as a black circle.

Generally, the data shows wide variance between observations using “identical” equipment that are only different by date and location. Since these are visual doubles, the time between measurements should not be a significant factor. The number of images in each data set range from 8 to 28 which should be sufficient for an accurate measurement. From the data in this investigation there is no clear explanation for the relatively wide variances has been identified as of this writing.

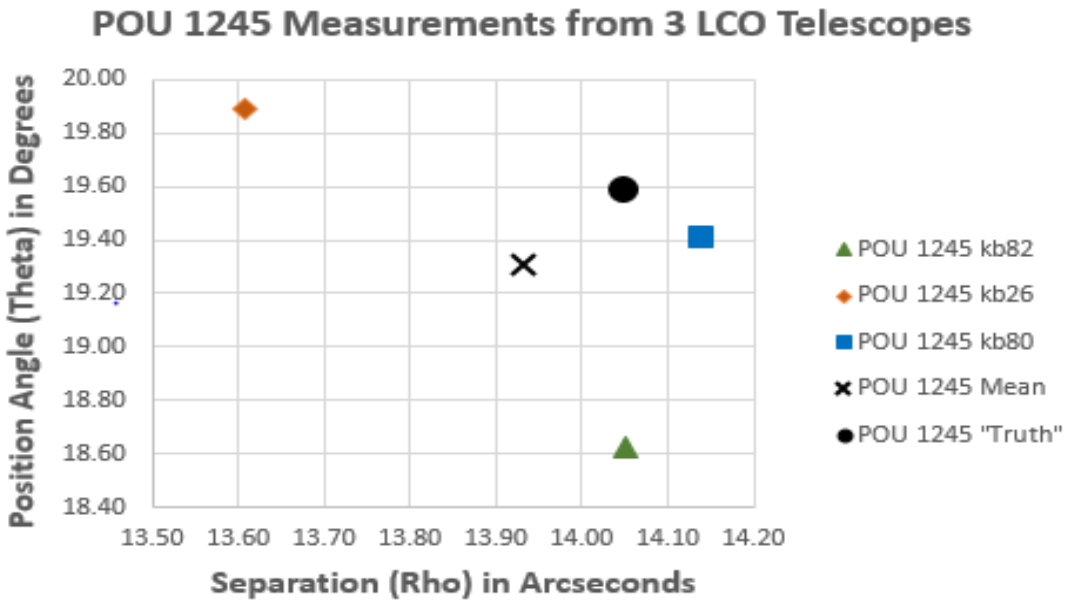

Figure 27. Plot of the rho and theta for POU 1245 as measured by "identical" LCO 0.4m telescopes in three different locations

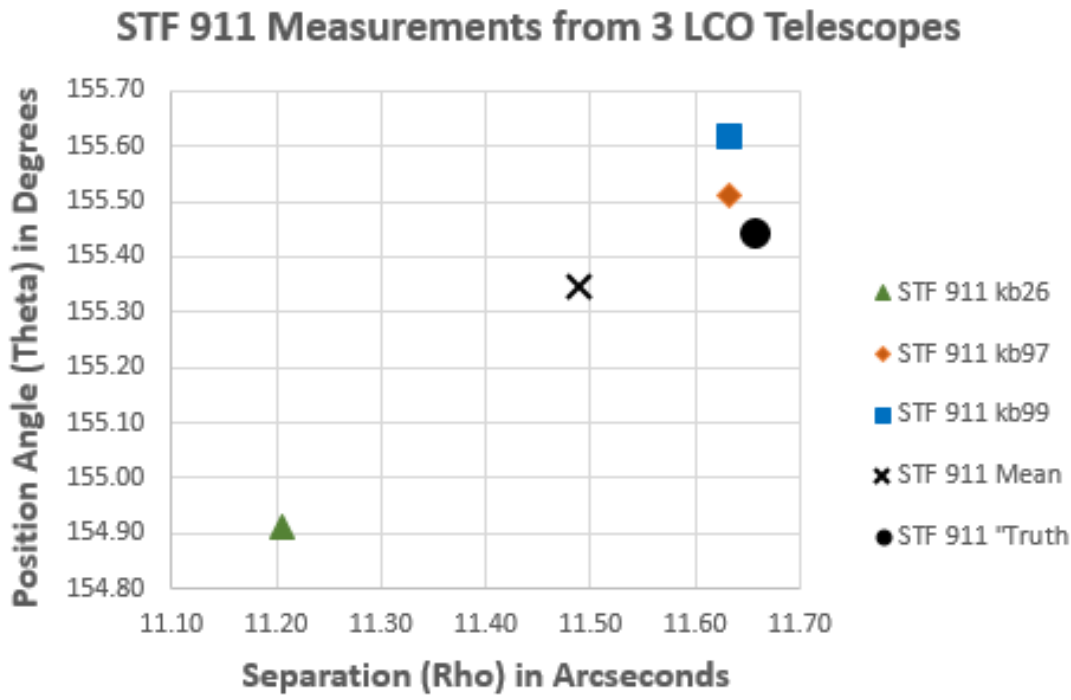

Figure 28. Plot of the rho and theta for STF 911 as measured by "identical" LCO 0.4m telescopes in three different locations

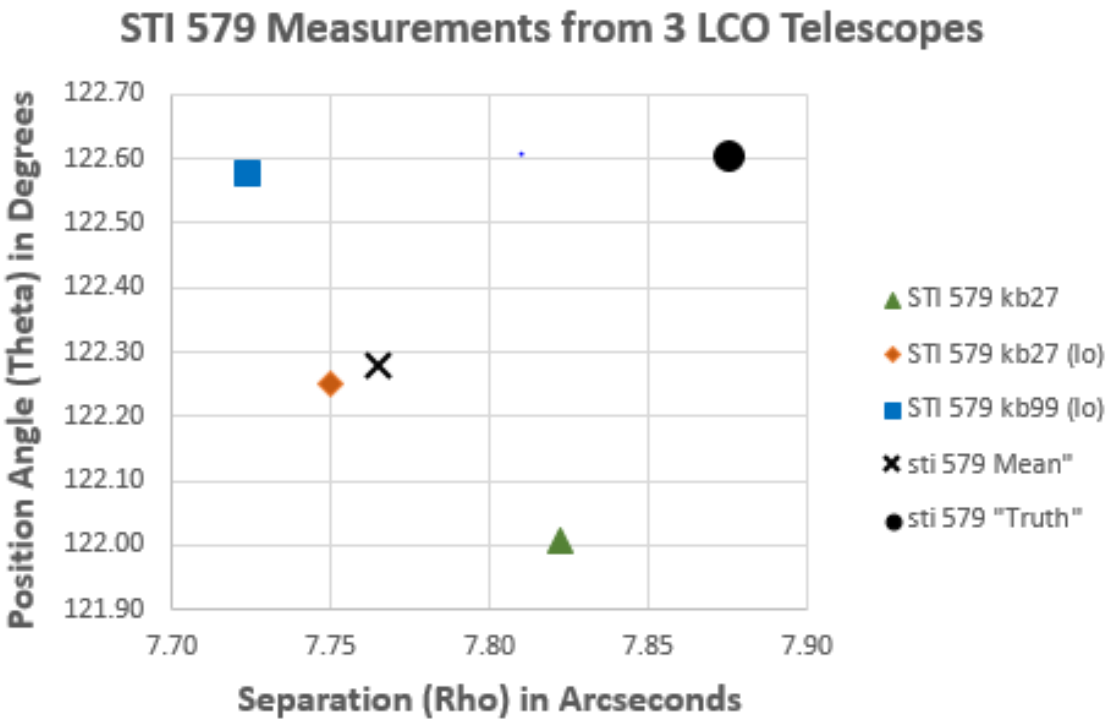

Figure 29. Plot of the rho and theta for STI 579 as measured by "identical" LCO 0.4m telescopes in three different locations

With serendipity, one might capture the better observation data set by chance. As with the logic of the night-to-night observations discussed above, one could argue that using multiple sites with "identical" equipment would improve certainty and may improve accuracy. Much more observation and analysis is required to understand these factors.

4.7 Data Reduction Methods

This investigation focuses on observational parameters that may affect double star measurements. One cannot ignore the impact of the data reduction tools and practices on the final product: an accurate and certain measurement. A very limited analysis of these methods on the product was performed. This is only a quick assessment to see make a judgment on how significant a factor the practices may be. The subject requires a full study and paper of its own to develop best practices.

One observation data set, STF 911 on January 5, 2018, using LCO kb97 (Siding Springs, Australia) was reduced by three different persons trained in using their specific data reduction tool: Mira Pro 64, SAO Image DS9, and AstroImage J (AIJ). The data set has 5 images each of green for 15 seconds, green for 30 seconds, red for 15 seconds, and red for 30 seconds for a total of 20 images. All of these images are saturated adding to the difficulty of making reliable measurements (see Figures 3, 4, and 5). More detailed information on the data set is in Table 7 in the Appendices. The measurement by other procedures helped to verify that the Mira Pro x64 measurements had not caused a distortion in this investigation.

The results from this very limited study as shown in Figures 30 and 31 indicate that the measurement tools procedure could be as significant as the observation tools and procedures in providing accurate measurements. A broad distribution of measurements from the same data is striking. The high SEM for DS9 is troubling and may warrant using other software or at least evaluating it.

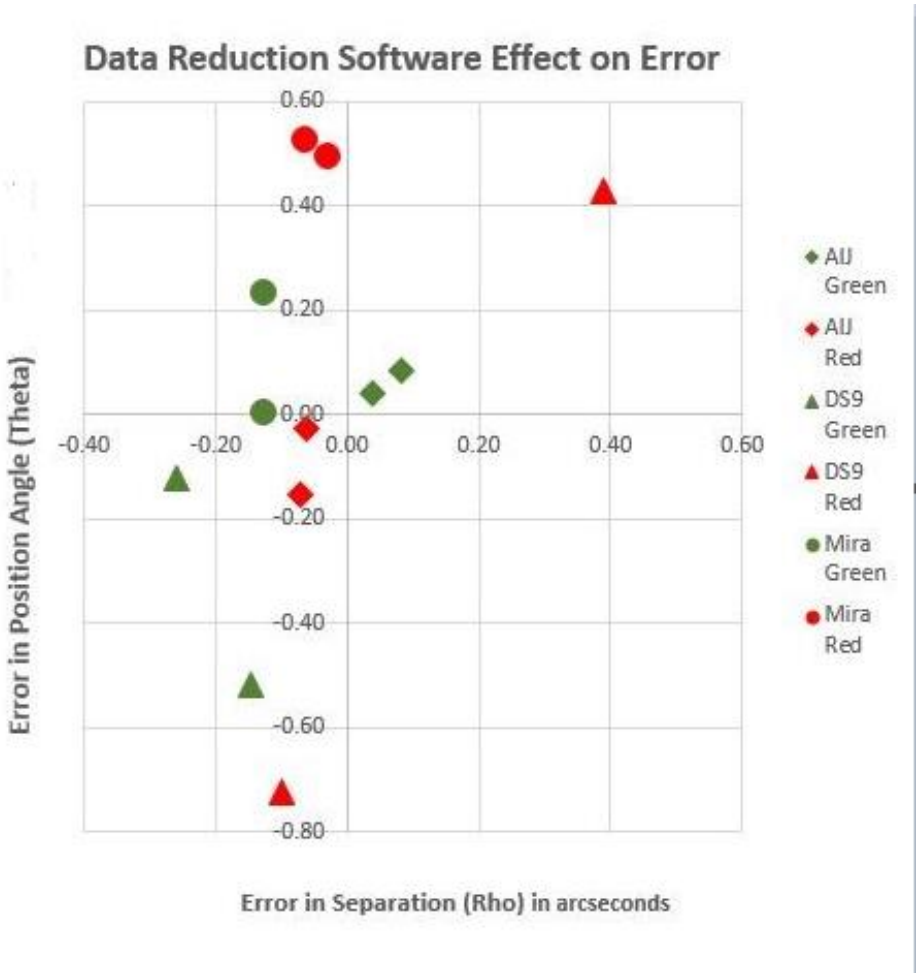

Figure 30. Plot of the mean errors in rho and theta for one detail observation set of STF 911 as measured by three different data reduction software products

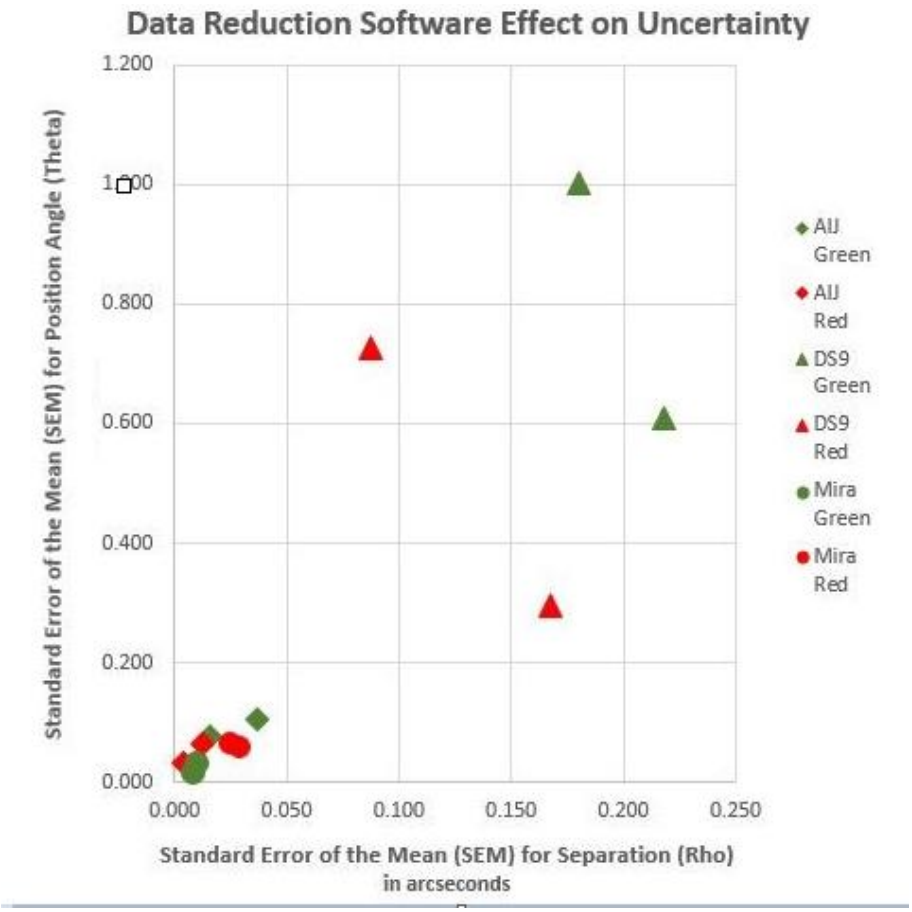

Figure 31. Plot of the standard error of the means in rho and theta for one detail observation set of STF 911 as measured by three different data reduction software products

5. Conclusions

This investigation explores a number of common questions raised by students doing research in BRIEF's DoubleSTARS seminars. Some of these preliminary results are unexpected and require further testing. Ongoing research will be conducted to refine, modify or confirm the findings in this paper. These and future results will inform the future DoubleSTARS research seminars and other astrometry research performed by Boyce-Astro students. The goal is to develop fact based "best practices" in measuring visual double stars and this study is already pointing to improvements.

BRIEF is making the data from this research available to the public in electronic form at its website: www.boyce-astro.org. All raw and processed data files are available at our public archive in raw FITS formats along with calibration files. Processed data, observation guides, analytics, and links to other publications associated with the research are also available in the archive.

BRIEF invites researchers interested in adding research content to the archive to contact the librarian at CIO@boyce-astro.org for further information.

6. Acknowledgements

The researchers gratefully acknowledge the comments and inspiration provided by Robert Buchheim over the past year in guiding the team toward the observation plan used in this investigation. The scope of the investigation would not have been possible in this time period without the benefits of the OSS Pipeline services provided to BRIEF by Michael Fitzgerald. Richard Harshaw and

Ed Wiley provided critical input especially on the importance of considering saturation in measuring double stars. Alex Falatoun supported the data reduction methods task as did Grady Boyce who assisted with review of documents and data. One cannot overlook the services provided by the Las Cumbres Observatory, iTelescope and the US Naval Observatory without which, this investigation would not be possible. And finally the researchers must acknowledge Boyce Research Initiatives and Education Foundation for sponsoring and funding the project.

7. References

Boyce, P. and Boyce, G., "A Community-Centered Astronomy Research Program" (2017). Proceedings of the Society for Astronomical Science.

Fitzgerald, M.T., "The Our Solar Siblings Pipeline: Tackling the data issues of the scaling problem for robotic telescope based astronomy education projects." (2018, accepted). Robotic Telescopes, Student Research and Education Proceedings.